Physikalisch-Technische Bundesanstalt

DECKBLATT

(PTB)

	Projekt	PSP-Element	Obj. Kenn.	Aufgabe	UA	Lfd Nr	Rev
	N A A N	N N N N N N N N N	N N N N N	X A A X X	A A	N N N N	N N
EU 340	9K	35212639		EGC	ED	0008	00

Titel der Unterlage:

Radionuklide chain transport in inhomogeneous crystaláne rocks: limited matrix diffusion and effective surface sorption

Seite: **I.**

Stand: **Feb. 1985**

Ersteller:

Swiss Federal Institute for Reactor Research

Textnummer:

Stempelfeld:

PSP-Element TP....**9K/21285**

zu Plan-Kapitel: **3.9**

PL

PL

V 89 / 788 / 1

Revisionsblatt

(PTB)

	Projekt	PSP-Element	Obj. Kenn.	Aufgabe	UA	Lfd. Nr.	Rev.
	N A A N	N N N N N N N N N	N N N N N	X A A X X	A A	N N N N	N N
EU 340	9K	35212639		EGC	ED	0008	00

Titel der Unterlage:

Radionuclide chain transport in inhomogeneous crystalline rocks: limited matrix diffusion and effective surface sorption

Seite: II.

Stand: Feb. 1985

Rev.	Revisionsst. Datum	verant. Stelle	Gegenzeichn. Name	rev. Seite	Kat. *)	Erläuterung der Revision

*) Kategorie R = redaktionelle Korrektur
Kategorie V = verdeutlichende Verbesserung
Kategorie S = substantielle Änderung
Mindestens bei der Kategorie S müssen Erläuterungen angegeben werden.

TECHNICAL REPORT 85-40

Radionuclide Chain Transport in
Inhomogeneous Crystalline Rocks:

Limited Matrix Diffusion and
Effective Surface Sorption

February 1985

Swiss Federal Institute for Reactor Research, Würenlingen

TABLE OF CONTENTS

VORWORT

Im Rahmen des Projektes Entsorgung werden im EIR Arbeiten zur Analyse der Ausbreitung radioaktiver Elemente aus einem Endlager durchgeführt. Diese Untersuchungen werden in Zusammenarbeit und mit teilweiser finanzieller Unterstützung der NAGRA vorgenommen. Die vorliegende Arbeit ist ein Referenzbericht im Rahmen des "Projektes Gewähr 1985" und erscheint gleichzeitig als EIR-Bericht und als Technischer Bericht der NAGRA.

ABSTRACT

In Switzerland high-level radioactive wastes are planned to be deposited in deep-lying crystalline formations. The present paper describes the modelling approach for geospheric nuclide transport in inhomogeneous crystalline rocks in the framework of a HLW safety assessment. The processes taken into account are advection and dispersion in water conducting structures which consist of a network of either fractures or veins embedded in dykes or kakirite zones, respectively. Out of these structures nuclides may diffuse into a spatially limited zone of altered crystalline. In addition sorption of nuclides on the rock is taken into account. Diffusion out of the fractures and sorption in the altered rock may often be represented by an effective surface sorption on the fracture walls. For transport of the 237-Np nuclide chain we present a sensitivity analysis taking a wide range of relevant parameters. The performance of the geologic barrier depends most critically on the extent of the altered zones.

Zusammenfassung

Es ist in der Schweiz geplant, hochradioaktive Abfälle in tiefliegenden Kristallinformationen einzulagern. Diese Arbeit beschreibt die Modellansätze zum geosphärischen Nuklidtransport in inhomogenem kristallinem Gestein im Rahmen der Sicherheitsanalyse für HAA. Die berücksichtigten Prozesse sind Advektion und Dispersion in wasserführenden Strukturen. Diese bestehen aus einem Netzwerk von Spalten oder Adern welche in Gesteinsgänge oder Kakiritzonen eingebettet sind. Nuklide können aus diesen Strukturen in ein räumlich begrenztes Gebiet verwitterten Kristallins diffundieren. Zusätzlich wird die Sorption von Nukliden am Gestein berücksichtigt. Die Diffusion aus den Spalten und die Sorption im verwitterten Gestein kann oft durch eine effektive Sorption an den Spaltoberflächen dargestellt werden. Für den Transport von 237-Np und seiner Zerfallsprodukte führen wir eine Sensivitätsanalyse durch, wobei die wichtigen Parameter in einem weiten Bereich variiert werden. Die Wirkung der geologischen Barriere hängt kritisch von der räumlichen Ausdehnung der Verwitterungszonen ab.

Résumé

En Suisse il existe le projet de stocker des déchets hautement radioactifs dans des formations cristallines profondes. La présente étude decrit les équations de modelisation du transport géosphérique des nuclides dans des roches cristallines inhomogènes, dans le cadre de l'analyse de sécurité pour DHA. Les procéssus considérés sont l'advection et la dispersion dans des structures conductrices d'eau. Celles-ci consistent d'un réseau de failles ou de veines, dans des intrusions ou de zones de kakirite. A partir de ces structures les nuclides peuvent diffuser dans une région de cristallin alterée limitée dans l'espace. Additionellement, la sorption des nuclides dans la roche est considérée. La diffusion à partir des failles et la sorption dans la roche alterée peuvent souvent être représentées par une sorption effective sur la surface de la faille. Pour le transport du 237-Np et de ses produits de désintégration nous effectuons une analyse de sensitivité, où les paramètres importants varient dans une large domaine. L'effet des barrières géologiques dépend de façon très critique de l'étendue spatiale des zones alterées.

1. INTRODUCTION

High-level radioactive wastes are planned to be deposited in deep-lying geologic formations. The objective of this disposal option is to guarantee that no or only acceptably small amounts of radionuclides reach the biosphere over time. It is generally agreed that transport by water through the geologic medium is the principal scenario since water access to the repository cannot be excluded and integrity of waste canisters and matrix cannot be assumed over thousands or even millions of years. The effect of the geologic barrier is twofold: it provides retardation mainly through sorption and dilution if substantial aquifers are present. Hence, radionuclide transport models are an important part in safety analyses for radioactive waste repositories.

The host rock under consideration in Switzerland is crystalline overlayed by a series of sedimentary rocks. Deep drill hole measurements show /1, 2/ that the crystalline is inhomogeneous and water conducting zones can be found in kakirites and aplite/pegmatite dykes. Water flow takes place in veins and fractures, respectively, embedded in these zones. The kakirites themselves and a small layer adjacent to the fractures in the dykes form zones of altered rock into which transported radionuclides may diffuse and being sorbed. Besides a differing geometry (for transport in kakirites) the present modeling approach differs from previous ones (e.g. /3, 4/) in that it takes into account diffusion into these limited zones of altered rock (limited matrix diffusion), only. The main reason behind this is that porosity in the altered zones is much higher than in the intact crystalline rock /2/ and an unambiguous validation of matrix diffusion in undisturbed rock is still lacking (see e.g. /5/).

The paper is organized as follows:

In the next section we present the models for transport in idealized veins and fractures, respectively. Processes taken into account are advection, hydrodynamic dispersion, limited matrix diffusion, sorption and radioactive decay and build-up. For transport in fractures an effective surface sorption retardation factor is defined and its validity discussed. The models presented have been extensively used in the recent safety assessment for a proposed Swiss repository for high-level wastes /6/.

In section 3 extensive numerical results are presented taking as an example the migration of the 237-Np chain. Starting from parameters deemed realistic within "Projekt Gewaehr 1985" /1/ variations are performed for both of the transport systems. The important parameter dependencies are exhibited.

Section 4 summarizes the conclusions and specifies some important open problems. It reiterates the need for further systematic experiments.

The appendix, finally, gives the salient features of the numerical solution of the transport equations. In addition it presents some results on numerical code verification.

2. THE SYSTEM OF TRANSPORT EQUATIONS

2.1 General

The transport equations are given by considering the mass balance for a representative elementary volume (REV) /7/. The quantities entering this mass balance are averages over the REV and hence macroscopic. The definition of a REV is not trivial and strongly depending on the transport system to be modelled. In the next subsections we will introduce two specific REVs approximating two different transport systems in inhomogeneous crystalline rocks.

Quite generally we distinguish three different zones in the crystalline rock. First are the water conducting structures. These might be systems of fractures or veins. The first are essentially planar structures whereas the second are more or less linear. In these zones we take into account advection of radionuclides, hydrodynamic dispersion and sorption on their surfaces. The second type are altered zones adjacent to the water conducting zones. In these, advection of contaminant can be neglected. However, diffusion and sorption in the altered rock are important processes. The third, and generally largest part of deep crystalline is intact rock. In view of its much lower hydraulic conductivity (orders of magnitude less than the altered zone /2/), its much lower porosity (0.2% compared to 3% of the altered zone /2/) and the open question of the existence of an extended network of connected pore space it is wise to neglect this part of the crystalline rock in transport calculations for safety purposes. We are thus left with a medium of double porosity and call this approach limited matrix *) diffusion.

Consider now a species i with concentrations in liquid phase, c^i,

and solid phase, S^i, and let us denote quantities in the water conducting system by an index f and in the altered zones by an index p, respectively. The transport equations are then given for the water conducting system by

$$\frac{\partial}{\partial t} (\varepsilon_f \, c_f^i + \delta_f \, S_f^i) = \vec{\nabla} \cdot \varepsilon_f \, \{D_f \, \vec{\nabla} \, c_f^i - \vec{v}_f \, c_f^i\} +$$

$$\varepsilon_f \, \varepsilon_p \, \frac{d\vec{F}}{dV_f} \cdot D_p \, \vec{\nabla} \, c_p^i + Q_f^i \quad , \tag{2.1}$$

and for the altered zones by

$$\frac{\partial}{\partial t} \{\varepsilon_p \, c_p^i + (1-\varepsilon_p)\rho \, S_p^i\} = \vec{\nabla} \cdot \varepsilon_p \, D_p \, \vec{\nabla} \, c_p^i + Q_p^i \quad . \tag{2.2}$$

The left hand side of the equations describes the variation with time of the total concentration. The first term on the right hand side is the divergence of a flux. In the water conducting system this is composed of a component from hydrodynamic dispersion (dispersion tensor D_f) and from advection (water flow field $\vec{v}_f$). The third term is ensuring flux continuity at the interface matrix / water conducting system ($\frac{dF}{dV_f}$ is the surface per volume of water conducting zone). In the altered zone molecular diffusion (diffusion tensor D_p) is taken into account, only. The terms Q^i are general net source terms describing reactions between different species i. Furthermore, ε_f is

----

*) In the following the term matrix is meant synonymous with altered zone.

the flow porosity, ε_p the matrix porosity, δ_f the surface of water conducting zones to volume ratio, and ρ the rock density.

2.2 Approximations

Equations (2.1) and (2.2) have to be solved with appropriate boundary and initial conditions. Before specifying these let us first introduce some approximations. These are motivated by a rather vaguely defined combination of the consequences of lack of data, judgment on the conservatism of the approach chosen and ease of the equation's solution. In principle, eqs. (2.1) and (2.2) as well as the approximations have to be validated. This has been done partially, only, and constitutes a major task for future research.

2.2.1 Species

We assume that the transport of each radionuclide can be described by the transport of an effective single species of this nuclide. This neglects the influence of kinetic speciation in liquid and solid phase. Of major concern, here, is the influence of colloids (see e.g. ref. /8/). Whereas for simple systems (single porosity medium, first-order kinetics) the validity of this approximation can be estimated /9/, the situation might be strongly different when matrix diffusion becomes important /10/. At present, data on formation, stability, filtration and sorption behaviour of colloids are lacking and we are neglecting their influence. The source terms then become

$$Q_f^i = -\lambda_i \, (\varepsilon_f \, c_f^i + \delta_f \, s_f^i) + \lambda_{i-1} \, (\varepsilon_f \, c_f^{i-1} + \delta_f \, s_f^{i-1}) \quad , \tag{2.3}$$

and

$$Q_p^i = -\lambda_i \, \{\varepsilon_p \, c_p^i + (1-\varepsilon_p)\rho \, s_p^i\} - \lambda_{i-1} \, \{\varepsilon_p \, c_p^{i-1} + (1-\varepsilon_p)\rho \, s_p^{i-1}\} \quad , \tag{2.4}$$

for a nuclide chain 1 --> 2 -->...--> i-1 --> i -->..., where λ_i is the decay contant.

2.2.2 Sorption

We assume instantaneous sorption equilibrium and a linear relationship between concentrations in liquid and solid phase. Though this is hardly an accurate description of nature /11/ the distribution constants can always be chosen conservatively, be it at the expense of strongly overestimating fluxes at the geosphere outlet /12/. Hence, we have the following relationship

$$s_f^i = K_a^i \, c_f^i \quad , \tag{2.5}$$

and

$$s_p^i = K_d^i \, c_p^i \quad , \tag{2.6}$$

where K_a^i and K_d^i are the surface and volume based sorption equilibrium distribution constants, respectively.

2.2.3 Dimensionality

We assume that advective nuclide transport *) in the water
conducting zones is one-dimensional along a trajectory given by
hydrology and neglect transversal dispersion, i.e. we consider
transport in a flow tube along a trajectory. Though this might not be
conservative in all cases /13/, it certainly is in the context of the
Swiss safety assessment "Project Gewaehr 1985" /1, 6/. In principle
the one-dimensional approach can be validated by comparing with two-
and three-dimensional calculations. For specific transport systems
this has been done in the framework of INTRACOIN /14/ with .sufficient
success /15, 16/. For this approximation, the water velocity reduces
to a single component v_f along a given water trajectory and the tensor
of mechanical dispersion to a single scalar which we write

$$D_f = a_L v_f \quad , \qquad\qquad (2.7)$$

where a_L is the longitudinal dispersion length. Here, we neglect
molecular diffusion because it is small and its effect could be
incorporated into the dispersion length whose value is uncertain,
anyway.

In the matrix we consider diffusion perpendicular to the water
conducting zones, only. This is justified since transport in these
zones is much faster than in the matrix.

----

*) It is in order to mention here that from the very beginning, eqs.
   (2.1) and (2.2), we have decoupled hydraulics and nuclide
   transport. For a repository in crystalline and the present
   knowledge of deep crystalline hydrology in Switzerland this is a
   sensible approximation.

2.2.4 Parameter variability in space and time

Time dependencies of parameters are not taken into account. In view of the long time scales to be considered, this is certainly a gross oversimplification for most of them: decay constants are an exception. Since little is known on time evolution of important parameters like sorption or spatial extent of altered zones a broad parameter variation must be done.

Spatial dependencies in the water conducting system are modelled by piecewise constant parameters. This defines a series of segments along the transport path. Radionuclide flux conservation at the segment interfaces requires continuity of the flux

$$- q \ (a_L \ \frac{\partial c_f^i}{\partial z} - c_f^i) \ , \tag{2.8}$$

where q is the specific discharge, and water mass conservation at the segment interfaces in the framework of a flow tube model with constant cross section requires continuity of

$$q \ c_f^i \ . \tag{2.9}$$

Provided q is unsteady at a segment interface, the ratio of specific discharges of the two adjacent segments defines a dilution factor.

2.3 Transport in Kakirite Zones

Kakirite zones are a result of tectonic activity resulting from the global stress field. The crystalline has been crushed and

altered in the hydrothermal phase. These zones are essentially planar structures with a thickness, 2D, of 10's of centimeters to a few meters and with welldefined dip and strike angles. Water transport is in veins which may be partially quartz covered. In a few laboratory experiments it has been shown that this quartz covering is interspersed with fractures /2/ and does not present a diffusion barrier to the altered crystalline /2, 17/. The veins are modelled as tubes with a fixed radius R and the effect of a network of veins is taken into by a longitudinal dispersion length a_L. The resulting model REV is depicted in fig. 1a.

The transport equations are given by

$$R_f^i \frac{\partial}{\partial t} c_f^i = a_L v_f \frac{\partial^2 c_f^i}{\partial z^2} - v_f \frac{\partial c_f^i}{\partial z} + \frac{2}{R} \varepsilon_p D_p \left. \frac{\partial c_p^i}{\partial r} \right|_{r=R}$$

$$(2.10)$$

$$- \lambda_i R_f^i c_f^i + \lambda_{i-1} R_f^{i-1} c_f^{i-1} \quad ,$$

and

$$R_p \frac{\partial}{\partial t} c_p^i = D_p \left\{ \frac{\partial^2 c_p^i}{\partial r^2} + \frac{1}{r} \frac{\partial c_p^i}{\partial r} \right\} - \lambda_i R_p^i c_p^i +$$

$$(2.11)$$

$$\lambda_{i-1} R_p^{i-1} c_p^{i-1} \quad , r > R \ .$$

Here, we have defined the retardation factors by

$$R_f^i = 1 + \frac{2}{R} K_a^i \quad , \tag{2.12}$$

and

$$R_p^i = 1 + \frac{(1-\varepsilon_p)}{\varepsilon_p} \rho K_d^i \quad . \tag{2.13}$$

The z-axis is along the tube, i.e. along the water trajectory, and the r-axis perpendicular to the tube axis.

The <u>initial condition</u> is given by

$$c_f^i (z,t) = c_p^i (r,t) = 0 \quad \text{for} \quad t \leq 0 \quad . \tag{2.14}$$

The <u>boundary conditions</u> are as follows:

At the interface tube/rock matrix we have

$$c_f^i (z,t) = c_p^i (R,t) \quad \text{for all } z \tag{2.15}$$

At the geosphere inlet we take

$$c_f^i (0,t) = c_0^i (t) \quad , \tag{2.16}$$

where c_0^i (t) is some arbitrary function, determined by the near-field release model (e.g. a solubility limit), and

$$c_p^i (r,t) = 0 \quad \text{for} \quad z = 0 \quad \text{and} \quad r > R \; . \qquad (2.17)$$

This last equation *) is consistent with neglect of the angular diffusion component in the altered zone.

Downstream, we take

$$c_f^i (\ell,t) = 0 \; , \qquad (2.18)$$

where ℓ is the migration distance in the kakirite zone. This boundary condition models the strong dilution in the aquifers overlaying the host rock in the Swiss repository concept. Diffusion into the kakirite is limited by the extent of that zone and the boundary condition is

$$\left. \frac{\partial c_p^i}{\partial r} \right|_{r=D} = 0 \; , \qquad (2.19)$$

assuming a tube in the center of the kakirite and sufficient distance to the next one. If, in a cross-sectional area of $4D^2$ there are n^2

----

*) We have also considered another choice, namely

$$c_p^i (r,t) = c_0^i (t) \quad \text{for} \quad z = 0 \quad \text{and} \quad r > R \; . \qquad (2.17a)$$

Both, eqs. (2.17) and (2.17a), give essentially the same fluxes at the geosphere outlet.

tubes we have from symmetry reasons

$$\left. \frac{\partial c_p^i}{\partial r} \right|_{r=D/n} = 0 \quad . \tag{2.19a}$$

Analytical solutions to eqs. (2.10) to (2.19) are not known to the authors.

2.4 Transport in Fracture Zones

Aplite and pegmatite structures /2/ have been formed during cooling down of the crystalline in the early hydrothermal phase. They form dykes of roughly the same width as the kakirites and are, though not regularily, roughly perpendicular to the kakirites. Water transport is in fractures with an adjacent small zone of altered material. Little is known on the frequency of water conducting fractures. However, the width of the altered zone, again denoted by D, is certainly much smaller than the distance s between fractures. The fractures are modelled as parallel water conducting zones with half-width b and the effect of a fracture network and dispersion within the fracture plane is taken into account by a longitudinal dispersion length a_L. The resulting model REV is depicted in fig. 1b.

The transport equations are given by

$$R_f^i \ \frac{\partial}{\partial t} \ c_f^i \ = \ a_L \ v_f \ \frac{\partial^2 c_f^i}{\partial z^2} \ - \ v_f \ \frac{\partial c_f^i}{\partial z} \ + \ \frac{1}{b} \ \varepsilon_p \ D_p \ \frac{\partial c_p^i}{\partial x}\bigg|_{x=b} \tag{2.20}$$

$$- \lambda_i \ R_f^i \ c_f^i \ + \ \lambda_{i-1} \ R_f^{i-1} \ c_f^{i-1} \quad ,$$

and

$$R_p^i \ \frac{\partial}{\partial t} \ c_p^i \ = \ D_p \ \frac{\partial^2 c_p^i}{\partial x^2} \ - \ \lambda_i \ R_p^i \ c_p^i \ +$$

$$\tag{2.21}$$

$$\lambda_{i-1} \ R_p^{i-1} \ c_p^{i-1} \quad , \quad |x| > b \quad .$$

The retardation factor R_p^i is given by eq. (2.13), whereas

$$R_f^i \ = \ 1 \ + \ \frac{1}{b} \ K_a^i \tag{2.22}$$

for this transport system. Again, the z-axis is along the water trajectory within the fracture plane, and the x-axis is perpendicular to this plane.

The initial condition is

$$c_f^i \ (z,t) \ = \ c_p^i \ (x,t) \ = \ 0 \quad \text{for} \ \ t \leq 0 \quad . \tag{2.23}$$

The boundary conditions are as follows:

At the interface fracture/rock matrix we have

$$c_f^i \ (z,t) \ = \ c_p^i \ (b,t) \quad \text{for all } z \ . \tag{2.24}$$

At the geosphere inlet eq. (2.16) holds and, again,

$$c_p^i (x,t) = 0 \quad \text{for} \quad z = 0 \quad \text{und} \quad x > b \tag{2.25}$$

is taken. The downstream boundary condition is given by eq. (2.18). Diffusion into the rock matrix is limited to the adjacent altered zone. Consequently we have

$$\left. \frac{\partial c_p^i}{\partial x} \right|_{x=D} = 0 \; . \tag{2.26}$$

2.4.1 Analytical solutions

Analytical solutions to the transport problem, eqs. (2.20) to (2.26) are not known to the authors. For simplified problems, however, analytical solutions have been presented. We mention two extremes:

Sudicky and Frind /18/ consider a single transported stable species (and without loss of generality D=s/2). They consider an infinite medium ($\ell = \infty$) and a constant upstream boundary concentration $C_0(t) = C_0$. The solutions can be written down in terms of a series of folding integrals. The numerical evaluation seems to require a major effort.

Another possibility is to simplify the problem to such an

extent that simple solutions emerge /19-21/. Let us neglect dispersion in the fracture, $a_L = 0$, take an infinite medium, $\ell = \infty$, a simple upstream boundary condition, $C_0(t) = C_0 e^{-\lambda t}$, and consider a single decaying species, only. Furthermore, we assume that the width of the altered zone (and the fractures' distance) is very large and the fracture half-width very small compared to the penetration depth into the matrix. Then, the solution in the fracture is given by

$$C_f(z,t) = \begin{cases} 0 & , \ t < \alpha \\ \\ C_0 \ e^{-\lambda t} \ \text{erfc} \sqrt{\dfrac{\tau_0}{t-\alpha}} & , \ t \geq \alpha \end{cases} \qquad (2.27)$$

and in the matrix by

$$C_p(x,t) = \begin{cases} 0 & , \ t < \alpha \\ \\ C_0 \ e^{-\lambda t} \ \text{erfc} \ \dfrac{\sqrt{\tau_0} + \dfrac{x}{2}\sqrt{\dfrac{R_p}{D_p}}}{\sqrt{t - \alpha}} & , \ t \geq \alpha \end{cases} \qquad (2.28)$$

where

$$\tau_0 = (\frac{z}{2b} \frac{\varepsilon_p}{v_f})^2 R_p D_p \quad , \qquad (2.29)$$

and

$$\alpha = \frac{R_f z}{v_f} \quad . \qquad (2.30)$$

If we define a break-through time t_0 by $C_f(z, t_0) = 1/2 \, C_0 \, e^{-\lambda t_0}$.
we see that

$$t_0 \approx \alpha + 4\tau_0 \quad . \qquad (2.31)$$

The parameter α describes retardation through sorption on the fracture surfaces, the parameter τ_0 retardation through diffusion (and sorption) into the rock matrix. Similarily, we define a penetration depth x_0 through $C_p(x_0, t) = 1/2 \, C_0 \, e^{-\lambda t}$ and obtain

$$x_0 = \sqrt{\frac{D_p}{R_p}} \{ \sqrt{t - \alpha} - 2\sqrt{\tau_0} \} \quad , \qquad (2.32)$$

which near the geosphere inlet simplifies to $x_0 \approx \sqrt{D_p t / R_p}$.
As a typical example take $D_p = 1.5 \cdot 10^{-10} \, m^2/s$ and $R_p = 1 \cdot 10^5$, then at a time of 10^3 yr we have $x_0 < 7$ mm. This shows the difficulties when trying to validate the matrix diffusion process.

2.4.2 Effective surface sorption

When diffusion into the altered zone is sufficiently fast, such that $C_f^i = C_p^i$ throughout the medium is a good approximation, it is evident from mass balance that the system of eqs. (2.20) and (2.21) reduces to

$$\bar{R}_f^i \; \frac{\partial}{\partial t} \; C_f^i = a_L \, v_f \; \frac{\partial^2 C_f^i}{\partial z^2} - v_f \; \frac{\partial C_f^i}{\partial z} - \lambda_i \, \bar{R}_f^i \, C_f^i$$

$$\quad (2.33)$$

$$+ \; \lambda_{i-1} \cdot \bar{R}_f^{i-1} \, C_f^{i-1} \quad ,$$

with an effective surface retardation constant

$$\bar{R}_f^i = 1 + \frac{1}{b} \; \{K_a^i + (1-\varepsilon_p)\rho \, D \, K_d^i\} \quad . \quad (2.34)$$

We will now give arguments <u>under which conditions</u> eqs. (2.33) and (2.34) are reasonable approximations. We consider a single decaying species, only, and define the functions

$$G = e^{\lambda t} \, C \quad . \quad (2.35)$$

Then, by Laplace transformation methods, it can be shown /22/ that the derivative of the coupling term in eq. (2.20) can be written

$$\frac{\partial G_p}{\partial x}\bigg|_{x=b\gtrless 0} = - \frac{R_p}{D_p} D \frac{\partial}{\partial t} \{ G_f - \frac{1}{6} \frac{R_p}{D_p} D^2 \frac{\partial}{\partial t} G_f + \text{higher derivatives} \} . \quad (2.36)$$

Assuming

$$K_d (1 - \varepsilon_p)\rho \gg \varepsilon_p \quad , \quad (2.37)$$

and retaining the first term, only, one arrives at eqs. (2.33) and (2.34). For steady-state conditions only the first term in (2.36) has to be taken into account and eqs. (2.33) and (2.34) are rigorous as can also be seen from eq. (37) in ref. /18/. For non-steady state conditions

$$\left| \frac{1}{6} \frac{R_p}{D_p} D^2 \frac{\partial G_f}{\partial t} \right| \ll G_f \quad (2.38)$$

is required. This is certainly not fulfilled in the rising part of the breakthrough curve but it may extremely well be in the peak region provided the inlet concentration is different from zero sufficiently long times. As a typical example we take, again, the numbers of the last subsection and $D = 10^{-3}$ m corresponding to a small altered zone /2/, and get $(\Delta G_f /\Delta t) / G_f \ll 0.28$ yr^{-1} . Hence, for practical purposes in safety assessment eq. (2.33) is an excellent approximation.

3. NUMERICAL RESULTS AND DISCUSSION

Especially because of the influence of radioactive decay the effectiveness of a particular physico-chemical mechanism and the results of transport calculations are extremely dependent on parameter choices. As a starting point we take the parameters chosen /1/ within "Project Gewaehr 1985" for the Swiss high-level waste repository in deep crystalline. The nuclide independent parameters are given in table 1. For the present purposes it suffices to consider a single actinide chain, namely that starting with 237-Np:

237-Np --> 233-U --> 229-Th --> ...   .

The nuclide dependent parameters are shown in table 2. Sorption on the surfaces of the water conducting zones can be neglected in comparison to the strong retardation by sorption in the altered zone. Hence, for all calculations we take $R_f^i = 1$.

We remind the reader that water velocities v_f and retardation factors R_f are not independent quantities but connected through the porosity ε_f. Denoting (in one dimension) the hydraulic conductivity of the water conducting zone by K, the hydraulic gradient by $\nabla\phi$ and the specific discharge by q, the relations are

$$q = K \nabla \phi \qquad (3.1)$$

$$v_f = q / \varepsilon_f \qquad . \qquad (3.2)$$

In our models the porosity is given by

$$\varepsilon_f = \begin{cases} n' \pi R^2 & \text{for the kakirite zone} \\ \\ 2 \bar{n} \, b & \text{for the aplite/pegmatite dykes} \end{cases} \quad (3.3)$$

where n' is the number of tubes per unit kakirite cross section and $\bar{n}$ the number of fractures per unit dyke width. The release rates R_R^i (t) into the geosphere are given by figure 2 taken from ref. /23/. These take into account elemental solubility limits which explains a time dependency for U-233 and Th-229 where other isotopes contribute to the solubility limit. The boundary concentration is given by

$$c_0^i(t) = \frac{R_R^i(t)}{Q_L} \quad , \quad (3.4)$$

where Q_L is the total water flow through the repository. This quantity is equivalent to a normalized nuclide flow into the geosphere.

The results of the calculations are presented in terms of concentrations or total nuclide flows Q_f^i at the migration distance ℓ normalized to the water flow through the repository. The latter is given by

$$Q_f^i(t) = - \{ a_L \frac{\partial}{\partial z} c_f^i - c_f^i \}_{z=\ell} \quad (3.5)$$

----

*) With fixed specific discharge, the transport problem is independent of fracture aperture for sufficiently strongly sorbing species.

3.1 Transport in the Kakirites

3.1.1 Base case parameters

Figures 3 and 4 show the concentrations of 237-Np at various times in the water conducting zone as a function of distance from the inlet and in the kakirite zone as a function of radius at a distance of 60 m from the inlet, respectively. Negligible amounts of 237-Np reach the observation point (migration distance ℓ), only, and it is senseless to present normalized flows Q_f^i . This is also true for the daughters 233-U and 229-Th being in radioactive equilibrium to 237-Np at long times. For these parameters the inhomogeneous crystalline represents an extremely efficient geologic barrier. The mechanism giving rise to this result is diffusion into and sorption in the altered zone. As can be seen from figure 4, the kakirite zone behaves like a sponge sucking in nuclides and retarding their transport through the water conducting veins. At z=60 m the altered zone fills up with radionuclide up to times of 10^6 years, and then we have essentially a homogeneous distribution throughout the kakirite decreasing with time. Maximal concentrations in the veins are obtained at the end of the release period, at $2 \cdot 10^7$ yr (fig. 2).

3.1.2 Low distribution constants

Taking the set of low distribution constants and keeping all other parameters fixed changes the situation strongly since the sorption capacity in the kakirite is reduced. Normalized nuclide flows at the observation point are presented in figure 5. Still, retardation in the transport system is very effective and the

reduction of normalized outflow to inflow is many orders of magnitude since breakthrough times are several ten millions of years. The daughters are in radioactive equilibrium with 237-Np. Their flow is independent of the particular release rate into the geosphere.

For the parameter set chosen here the altered zone is faster equilibrated with radionuclides than for the previous one. The extreme effect of spatial extent of this zone is exemplified in figure 6. A reduction of kakirite width by a factor of five increases nuclide flow by roughly eight orders of magnitude. For the narrowest kakirite zone the geologic barrier reduces flow by a single order of magnitude, only. In fact, the highly nonlinear dependence of releases from the geosphere on the extent of the altered zone calls for the firm determination of relevant parameters and further validation of matrix diffusion.

3.1.3 Low diffusivity in the kakirite

Taking the lower diffusion constant in the kakirite and keeping all other parameters as in the base case yields the results presented in figure 7. Radionuclides are less mobile in the altered zone and effectively only parts of the kakirite zone contribute to retardation. Nevertheless reduction of normalized radionuclide flow for 237-Np is five orders of magnitude in the peak region. As a result of slowed-down diffusion into the kakirite the rising part of the curves is more pronounced. Because 229-Th is released at considerable quantities into the geosphere, up to 10^5 yr the inlet contribution to the outlet flow can clearly be seen. For larger times also this daughter is in radioactive equilibrium with its precursor.

3.1.4 High dispersion length

Taking the large dispersion length for transport in the water conducting veins and keeping all other parameters as in the base case yields the results shown in figure 8. Compared to the base case a larger amount of radionuclides is relatively rapidly transported through the geosphere and a broad time distribution for the normalized flows at the observation point results. The reduction in 237-Np flow is still seven orders of magnitude. The daughters 233-U and 229-Th are in radioactive equilibrium with this nuclide (A small deviation for 229-Th can be seen because of the reasons mentioned in the last subsection).

3.1.5 Combined parameter variations

First, we combine the set of low distribution constants with the small kakirite diffusion constant keeping all other parameters fixed. The results are shown in figure 9. Very roughly the results are similar to those of figure 7 emphasizing again the importance of diffusion in the kakirite zone. Break-through is somewhat earlier and the absolute magnitude higher. Both of this results from smaller sorption distribution constants which also leads to differing concentration ratios for the radioactive equilibrium situation at times larger than 10^7 years. The inflow contribution to outflowing 229-Th is pronounced: Because of small sorption an appreciable amount of inflowing nuclides survives geosphere transport. In this context it is interesting to note that break-through time for an inert tracer is 2400 yr *).

Second, we combine the small tube radius with the increased

tube frequency keeping all other parameters fixed. For a given water flux through ideal tubes, these two quantities are related, of course, by Hagen-Poiseuille's law. For a system of veins with varying cross section and surface roughness the relationship is unknown but it seems sensible to combine a decrease of tube radius with an increase of frequency. Comparing to the base case, though the water velocity v_f increases by a factor of 100/9, the kakirite zone is fully equilibrated with nuclides much faster because of the increased tube frequency. As a result normalized nuclide flows at the observation point are below 10^{-21} mol/l and hence negligible.

3.2 Transport in Fracture Zones

The results for calculations of transport in fracture zones are presented in figures 10 to 16. In all figures the normalized nuclide flows at the observation point (migration distance ℓ = 500 m) are presented as a function of time for both the full solution of limited matrix diffusion, eqs. (2.20) and (2.21) and the effective surface sorption approximation, eq. (2.33), respectively. In the rising part of the curves the results for effective surface sorption ly consistently somewhat lower. This is understandable since the approximation neglects kinetic effects of diffusion into the altered zone and assumes instantaneous equilibrium of concentrations in the water conducting zone with that in the altered zone. However, for the parameters chosen effective surface sorption constitutes an excellent approximation: For all but one single calculation (figure

---

*) Compare this, in addition, to the water transit time, ℓ/v_f = 83 yr, to again appreciate the effect of diffusion into the kakirite zone.

16) the results are identical within drawing accuracy over orders of
magnitude in nuclide flow.

3.2.1 Base case parameters

Figure 10 shows the normalized radionuclide flow when all
parameters are fixed as in the base case. The geologic barrier
performes much less effectively than for transport in the kakirite
zones (compare to figure 3). Flow reduction is three orders of
magnitude, only. This is caused by the much smaller extent of the
altered zone compared to the width of the kakirites. Hence, matrix
diffusion becomes much less effective. The daughters of Np-237 are in
radioactive equilibrium. The calculations with an effective surface
sorption are virtually indistinguishable from those with kinetic
matrix diffusion. We would like to mention that this is true, also,
when the width of the altered zone is increased to D = 0.01 m. For
this case retardation is much stronger and since normalized nuclide
outflows are less than 10^{-23} mol/l we do not show them explicitely.

3.2.2 Low distribution constants

The results for the set of low distribution constants and
keeping all other parameters fixed are shown in figure 11. For 237-Np
the geologic barrier produces essentially a retardation of a few
million years, only. At this time the daughter nuclides are in
radioactive equilibrium. At times around 100'000 years the inlet
contribution of 229-Th can be seen at a very low flow level. Also
here, effective surface sorption constitutes an excellent
approximation.

For this reason it is evident that when increasing the width of the altered zone to 0.01 m (figure 12) we regain the results of figure 10 for 237-Np (the increase in width is offset by the decrease in sorption constant). The results for the daughter nuclides, again being in radioactive equilibrium, have changed because of differing K_d-ratios.

3.2.3 Low fracture frequency

The results for the low fracture frequency and keeping all other parameters fixed are exhibited in figure 13. Because the specific discharge is kept fixed, water velocity v_f increases by a factor of 10. Here also, the geologic barrier causes a retardation for 237-Np, only, and the daughters are in radioactive equilibrium. Effective surface sorption is a very good approximation. For this reason the 237-Np results coincide with those of figure 11, the increase in water velocity being compensated by the decrease in sorption distribution constant.

3.2.4 Low diffusivity in the altered zone

Decreasing the diffusion constant in the altered zone by a factor of 10 leads to the same results as shown in figure 10 because surface sorption is a good approximation.

3.2.5 Combined parameter variations

For all these variations we have taken the low fracture frequency and the low diffusion constant in the altered zone in

order to be sensitive to the effective surface sorption approximation. The parameters to be varied in this subsection are sorption equilibrium constants, K_d, and width of the altered zone, D. All other additional parameters are kept fixed as in the base case.

First, we consider the set of high sorption constants (as in the base case) and a width of D = 0.01 m for the altered zone. The results are given in figure 14. Effective surface sorption is, once more, an excellent approximation and the results are the same as in figure 10. This is the case since the effect of decreased fracture frequency is compensated by the increase in width D by the same factor of 10. A further increase in the width to D = 0.1 m yields normalized nuclide outflows of less than 10^{-23} mol/l, a totally insignificant level.

Second, we take the set of low sorption constants. For the base case width of D = 0.001 m the results are presented in figure 15. Retardation is small in this case. 237-Np flow is not lowered by geologic transport. For 229-Th the inflow structure can clearly be seen (compare to figure 2) decay leading to a lowering of roughly an order of magnitude. Up to 200'000 years also the inflow contribution of 233-U can be recognized. Effective surface sorption is an excellent approximation.

Increasing, now, the width of the altered one to D = 0.1 m yields the results of figure 16. Normalized flows have droped by more than three orders of magnitude emphaszising again the importance of matrix diffusion and knowledge of the extent of altered zone. Roughly speaking the results are the same as in figure 12, the increase in water velocity being compensated by an increase in width

(both by a factor of 10). However, the e ective surface sorption approximation is not as good as in ι calculations considered hitherto. This can be understood when looking at eq. (2.38). This implies for 237-Np $(\Delta G_f/\Delta t)/G_f \ll 3.7 \cdot 10^{-5}$ yr^{-1}, requiring concentration variations of much less than 4% in 1000 years.

4. CONCLUSIONS

We have developed models for radionuclide chain transport in inhomogeneous crystalline rock. Advective and dispersive nuclide transport takes place in either one- or two-dimensional water conducting zones (veins or fractures, respectively). Out of these zones nuclides diffuse into the spatial limited zone of adjacent altered rock (kakirites or altered crystalline, respectively). We may call this mechanism limited matrix diffusion. For the case of transport in fractures *) we have investigated the conditions under which kinetic limited matrix diffusion can be represented by an instantaneous effective surface sorption.

Starting from site-specific parameter values as they are used for safety assessments within the Swiss "Projekt Gewaehr 1985" we have investigated the influence of various parameters on 'geologic barrier performance for two different systems, namely veins in kakirite zones and fractures in aplite/pegmatite dykes. The following conclusions can be drawn:

a) The most important parameter is the spatial extent of the zone of altered crystalline adjacent to the water conducting structures. Depending on its width radionuclide outflow may be totally insignificant or essentially come up to the inflow.

b) Transport in kakirites and aplite/pegmatite dykes differs strongly. This is less a consequence of different geometry of water

----

*) Though it is quite trivial to derive an effective surface sorption constant in the case of transport in tubes, provided $C_f = C_p$ for all z, we were unable to derive a relation equivalent to eq. (2.38) defining the range of applicability.

conducting zones but more a result of the point emphasized above.

c) A small value of the diffusivity in the altered zone resulting from tortuosity and constrictivity of the individual connected pores strongly reduces the retardation power of an extended altered zone.

d) Mechanical dispersion in the water conducting zones is realtively unimportant provided its value is not too large (less than a_L = 100 m in the present calculations, say). Though this is largely a free parameter we feel that a_L = 250 m is unphysically large.

e) It is known for decades, now, and needs not to be stressed especially that sorption is an efficient mechanism for retardation. For the present models the sorption capacity of the altered zones is particularily important. However, also non-sorbing nuclides are retarded to some extent.

f) For transport in the fractures limited matrix diffusion may be represented by an effective surface sorption. This reduces the numerical expenditure appreciably.

g) The numerical method of solution of the transport equations is efficient. In general, the rate of convergence to stable results in function of grid points is much faster than for conventional second order finite difference methods. Boundary conditions can be implemented as defined by the physical problem at hand.

Finally, we also want to mention some open problems:

a) Though not the topic of the present work, a better knowledge of parameters is indispensable. This implies systematic experiments in the field, in the laboratory and analogue studies.

b) The same is needed for further validation of model approaches. In this respect matrix diffusion is most crucial. Though diffusion into a limited zone of altered rock seems to be conservative it has to be validated in greater detail. In addition diffusion into the intact rocks could yield further retardation.

c) Transport of colloids needs to be considered. Little is known on their formation and stability, on their transport properties, especially the ability to diffuse into the pore space of the altered zones. Probably little is gained in realism of description without taking into account kinetic chemical reactions between colloids and dissolved ionic species.

d) The accumulating data suggest that non-linear sorption is the rule rather than the exception. In order to gain realism and reduce conservatisms non-linear isotherms have to be taken into account.

All these problems are interconnected and the importance of the first point as a "driving force and a yardstick" is emphasized in concluding.

APPENDIX

Numerical Solution of the Partial Differential Equations

We consider the numerical solution of the parabolic type partial differential equations (2.10), (2.11) and (2.20), (2.21), respectively, which we write in the form

$$\frac{\partial C}{\partial t} = a_1 C^{(2)} + a_2 C^{(1)} + a_3 C + a_4 S^{(1)} \bigg|_{r=R} + Q_1$$

$$= L_1 (C,S) + Q_1 \quad ,$$

(A.1a)

and

$$\frac{\partial S}{\partial t} = b_1 S^{(2)} + b_2 S^{(1)} + b_3 S + Q_2 = L_2(S) + Q_2 \quad ,' \qquad (A.1b)$$

with coefficients a_i and b_i which may be space and time dependent, satisfying $a_1, b_1 > 0$ and $a_3, b_3 \leq 0$. For convenience all indices have been omitted and the functions C_f^i and C_p^i are replaced by C and S, respectively. The derivatives are given in the notation

$$C^{(2)} = \frac{\partial^2 C}{\partial z^2} \quad , \quad S^{(2)} = \frac{\partial^2 S}{\partial r^2} \quad ,$$

$$\qquad (A.2)$$

$$C^{(1)} = \frac{\partial C}{\partial z} \quad , \quad S^{(1)} = \frac{\partial S}{\partial r} \quad .$$

We consider the solution of equation (A.1a) in the domain

$$0 < z < \ell \ , \ t > 0 \qquad \qquad \text{(A.3a)}$$

and of equation (A.1b) in the domain

$$R < r < D \ , \ t > 0 \qquad \qquad \text{(A.3b)}$$

together with the boundary conditions

$$C(0,t) \ = \ C_0(t) \qquad C(\ell,t) = 0 \qquad \qquad \text{(A.4a)}$$

$$S(R,t) \ = \ C(z,t) \qquad \forall z \qquad \qquad \text{(A.4b)}$$

$$S^{(1)}(r,t)\Big|_{r=D} \ = \ 0$$

for $t > 0$ and the initial conditions

$$C(z,0) = 0 \qquad \qquad 0 \le z \le \ell \qquad \qquad \text{(A.5a)}$$

$$S(r,0) = 0 \qquad \qquad R \le r \le D \qquad \forall z \qquad \text{(A.5b)}$$

The function $C(z,t)$ is required to be continuous for $z \epsilon \ [0,1]$, $t \ge 0$; also $C^{(2)}(z,t)$ and $\frac{\partial}{\partial t} C(z,t)$ are required to exist for $0 < z < \ell$, $t > 0$. The same condition holds for $S(r,t)$ for $r \epsilon \ [R,D]$ and every z value.

Due to the boundary condition (A.4b) which couples the function $C(z,t)$ with $S(r,t)$ the problem is two-dimensional in space in the sense that equation (A.1b) has to be solved for every z-value.

Among the various methods for the numerical solution of partial differential equations (PDE's) we use the method of lines /25/

approximation. The term "method of lines" is often used collectively to describe a large number of related techniques in which piecewise approximation polynominals in the spatial dimensions are used to transform PDE's into coupled ordinary differential equations sets. The basic objective of this method is thus a semidiscretization scheme where the space domain is represented by a set of discretely spaced points and the time is left continuous. Thus there are two basic steps that must be undertaken to obtain numerical solutions for eq. (A.1). One is to identify the means for approximating the spatial derivatives and the other is to select the procedure for time integration.

Spatial discretization

Assuming that the two dimensional integration domain is replaced by a set of mesh points given by

$$\{z\} = \{z_1, \ z_2, \ \dots z_N\}$$
$$\{r\} \quad \{r_1, \ r_2, \ \dots r_M\} \ ,$$

$$(A.6)$$

with spacings $dz_i = z_{i+1} - z_i$ and $dr_i = r_{i+1} - r_i$, the resulting rectangular space mesh system is defined as shown in figure A. The mesh points are labelled as indicated in the figure.

The semidiscretization involves a representation of the differential operators L_1 and L_2 at the given mesh points in terms of the functional values of $C(z,t)$ and $S(r,t)$. This can be done by Lagrange interpolation techniques /26/: given a set of data points $(x_1, f_1), \dots (x_K, f_K)$ where (x,f) may either denote (z,C) or (r,S)
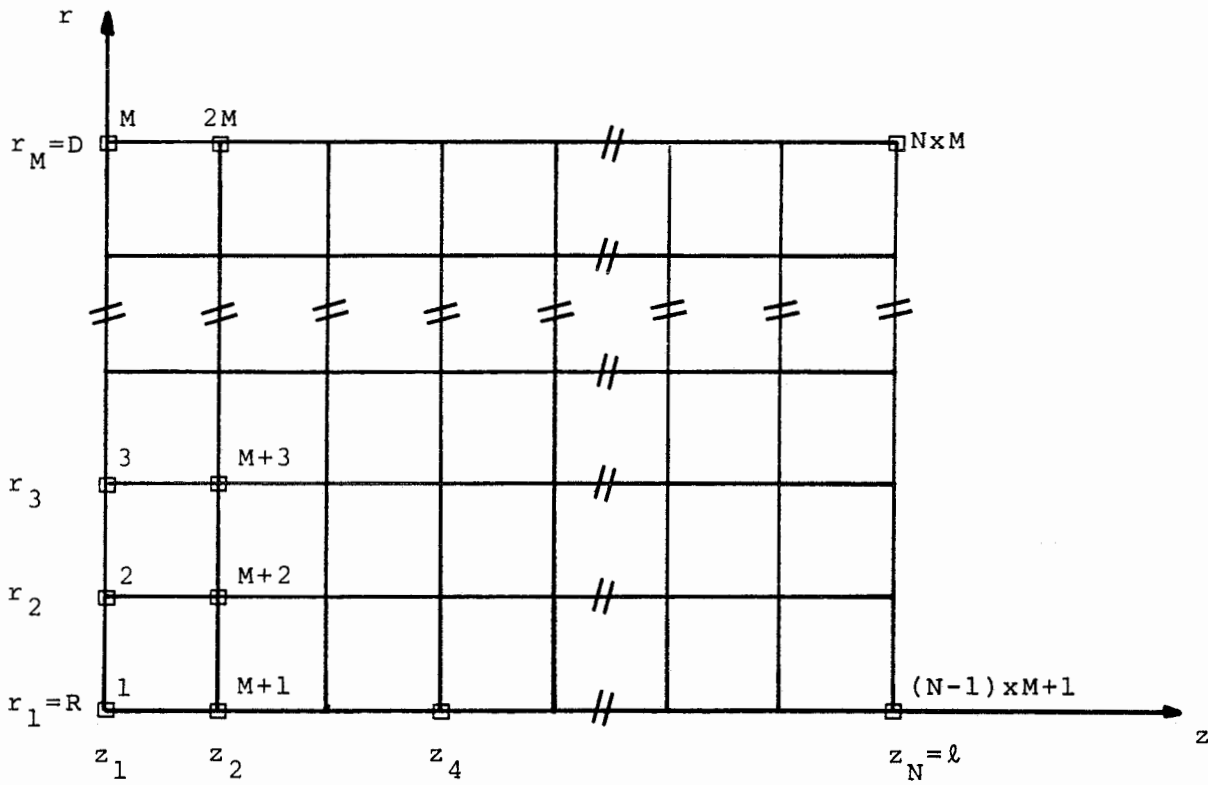
Figure A   Space mesh system

with $f_i = f(x_i, t)$ the $(K-1)$th order interpolation polynomial through

the points x_i is the interpolation polynomial given by:

$$P_{K-1}(x) = L_1(x)f_1 + L_2(x)f_2 + \dots L_K(x)f_K$$

$$= \sum_{i=1}^{K} L_i(x)f_i$$

(A.7)

where

$$L_i(x) = \frac{\prod\limits_{j=1}^{K} (x - x_j)}{\prod\limits_{j=1}^{K} (x_i - x_j)} \quad , \quad j \neq i$$

(A.8)

Since $L_i(x_j) = \delta_{ij}$ we have $P_{K-1}(x_i) = f_i$, and the polynomial represents the given data points. $P_{K-1}(x)$ is now used as approximation to the unknown function $f(x,t)$, i.e.

$$f(x) \simeq P_{K-1}(x) \tag{A.9}$$

Thus the first derivative is given by

$$f^{(1)}(x) = \sum_{i=1}^{K} L_i'(x) f_i \tag{A.10}$$

with

$$L_i'(x) = \frac{\sum\limits_{j=1}^{K} \prod\limits_{\ell=1}^{K} (x-x_\ell)}{\prod\limits_{j=1}^{K} (x_i-x_j)} \quad , \quad \begin{array}{l} j \neq i \\ \\ \ell \neq i,j \end{array} \tag{A.11}$$

and for the second derivative we find

$$f^{(2)}(x) = \sum_{i=1}^{K} L_i''(x) \cdot f_i \tag{A.12}$$

with

$$
L_i{}''(x) = \frac{\displaystyle\sum_{j=1}^{K} \sum_{m=1}^{K} \prod_{\ell=1}^{K} (x-x_\ell)}{\displaystyle\prod_{j=1}^{K} (x_i-x_j)} \quad , \quad \begin{array}{l} j \neq i \\[4pt] m \neq i,j \\[4pt] \ell \neq i,j,m \end{array} \tag{A.13}
$$

As an example we show the fourth order approximation for an uniform mesh with spacing h

$$
\xleftarrow{\quad} h \xrightarrow{\quad}
$$

$$
|\text{------}|\text{------}|\text{------}|\text{------}|\text{------}|\text{------}|\text{------}|
$$

$$
x_1 \qquad x_2 \qquad x_3 \qquad x_4 \qquad x_5 \qquad x_6 \qquad x_7 \qquad x_8
$$
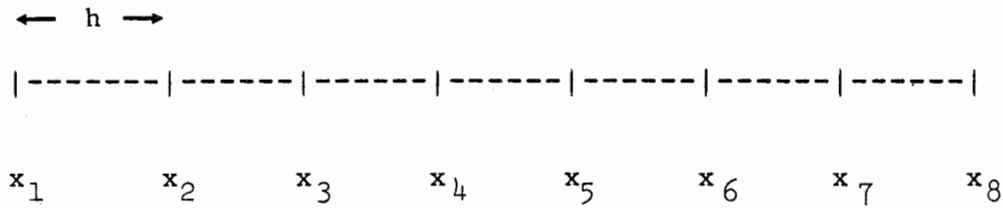
Then for example, the symmetrical approximation of $f^{(1)}$ is given by

$$
f^{(1)}(x_4) = \frac{1}{12h} (f_2 - 8f_3 + 8f_5 - f_6)
$$

$$
\tag{A.14}
$$

$$
f^{(1)}(x_5) = \frac{1}{12h} (f_3 - 8f_4 + 8f_6 - f_7)
$$

and for the second derivative $f^{(2)}$ we have

$$
f^{(2)}(x_4) = \frac{1}{12h^2} (-f_2 + 16f_3 - 30f_4 + 16f_5 - f_6)
$$

$$
\tag{A.15}
$$

$$
f^{(2)}(x_5) = \frac{1}{12h^2} (-f_3 + 16f_4 - 30f_5 + 16f_6 - f_7)
$$

representing the usual 4-th order central difference formulae. At the boundary points forward or backward formulae are used.

Using this approximation and defining according to the mesh numbering (c.f. Fig.A)

$$C(z_1,t) \quad = \quad f_1 \ , \quad C(z_2,t) \quad = \quad f_{M+1} \ , \quad \ldots \ C(z_N,t) = f_{(N-1) \cdot M+1}$$

$$S(r_2,t) \Big|_{z=z_1} = \quad f_2 \ , \quad S(r_3,t) \Big|_{z=z_1} = \quad f_3 \ , \quad \ldots \ S(r_M,t) \Big|_{z=z_1} = f_M \tag{A.16}$$

$$S(r_2,t) \Big|_{z=z_N} = \quad f_{(N-1) \cdot M+2} \ , \quad \ldots\ldots\ldots \ S(r_M,t) \Big|_{z=z_M} = \quad f_{N \cdot M}$$

we obtain an initial-value differential equation system of the form

$$\frac{df_i(t)}{dt} \quad = \quad \sum_{j=1}^{N \cdot M} \ V_{ij} \ f_j(t) + Q_j(t) \tag{A.17}$$

The values of the matrix elements depend on the order of approximation used and on the coefficients a_i and b_i in the differential equation (A.1). The structure of the matrix depends only on the order of approximation and on the ordering of mesh points (c.f. fig.A). Assuming a discretization with six matrix points and a second order approximation for the spatial derivatives the matrix V has the following form:

```
                        1 1 1 1 1 1 1 1 1 1 . . . .
    1 2 3 4 5 6 7 8 9 0 1 2 3 4 5 6 7 8 9 . . . .
   ------------------------------------------------
 1  x  x  x           x                 x
 2  x  x  x
 3     x  x  x
 4        x  x  x
 5           x  x  x
 6           x  x  x
 7  x                 x  x  x           x
 8                    x  x  x
 9                       x  x  x
10                          x  x  x
11                             x  x  x
12                             x  x  x
13                    x                 x  x  x           x
14                                      x  x  x
15                                         x  x  x
16                                            x  x  x
17                                               x  x  x
18                                               x  x  x
19
 .
 .
 .
```

(A.18)

The matrix V is of banded structure with two off-diagonal bands. The main band arises from the differential equation in the matrix and the upper and lower off-diagonal band from the equation for transport along the fracture. As the order is increased the number of upper and lower codiagonals in the diagonal band and the number of off-diagonal bands will increase. It should be mentioned, that this is not the only and probably not the best way of ordering the mesh points (the solution of the system of algebraic equations for the time integration may be become numerically instable). More compact structure of the matrix is possible which will be examined in future work.

Time integration

For the numerical integration of the coupled differential equations (A.17) we use Gear's backward /27,12/ method which is well appropriate if the system behaves as stiff. The stiffness depends on the eigenvalues μ_i of the Jacobian being in our case just the matrix V. The magnitude of the eigenvalues depends on the nature of the functions a_i and b_i in eq. (A.1) and on the discretization scheme. If the inequality

$$\max_{1 \leq j \leq N \cdot M} |\mu_j| \quad \gg \quad \min_{1 \leq j \leq N \cdot M} |\mu_j| \tag{A.19}$$

holds for the eigenvalues stiffness will occur and usual predictor-corrector methods or explicit methods will result in very small time step sizes.

In Gear's method as implemented in the IMSL library /28/ local error estimates, variable order approximation and variable step sizes are possible. Generally, time discretization errors are typically much smaller than are spatial discretization errors since the steps are restricted in size by explicit stability conditions.

However, one of the problems connected with the IMSL routine DGEAR is the fact that the solution scheme of the differential equation uses the Jacobian for which, however, only two different structures are considered: the full and the banded Jacobian case. Both of these are not economic either due to large computing times or large memory requirements. For typical applications the matrix V may be in the order of 600 x 600 where, however, only about thousand

matrix elements are non-zero. Thus the Yale sparse matrix solv r /29/ has been included in the Gear package to allow for sparse matrix structure.

Numerical results

For the numerical solution of coupled transport equations of the form (A.1) a program package RANCHMD has been developed which takes into account general initial and mixed boundary conditions. The transport equation is solved in the semidiscretized form (A.17) with variable order for the space derivatives.The integration of the differential equations is handeld by a modified version of the IMSL subroutine DGEAR. The choice of time step size is done automatically and controlled by the requested accuracy. A detailed program description is given in ref. 30.

The solution of the semidiscretized equations (A.17) may differ from the solution of the differential equation (A.1) for several reasons. First, the difference equation only approximates the differential equation and this introduces a truncation error which will vanish as dr and dz approaches zero. Second, the solution of the difference equation and differential equation may differ even in the limit as dt and dr,dz approache zero. This lack of convergence may be interpreted as instability of the semidiscretized equations:
llations in an erroneous fashion will occur. However, it can be shown by a von Neumann stability analysis that the discretization scheme chosen together with the backward Gear method is stable in the sense that the effect of an error introduced at any point does not increase as the computation proceeds with time, i.e. the solution

algorithm is stable.

However, even with a stable method, there are no mathematical criteria in choosing the space mesh sizes dr and dz in order to get useful solutions. Statements about step sizes and thus about accuracy of the solution can be done only by:

a) comparing numerical results with analytically solvable models or with results from other computer codes

b) performing calculations with varying step sizes dr and dz in order to test convergence of the solution.

Within the INTRACOIN project /31/ comparisons of type (a) have been done extensively /32/ in the case of a fractured system. The result produced with RANCHMD compare very well with numbers from analytically solvable models and with other computer codes. Care has to be taken with the order of spatial approximation and with the mesh spacing dr and dz. They depend on the magnitude of the values of a_i and b_i in eq. (A.1).

Thus, for our calculations we examined the convergence behaviour of the numerical solution in function of the mesh sizes for some typical parameters used.

As an example for the fractured system, we show in fig. A.1 for the parameter variation

$$v_f = 4.73 \text{ m/yr} \qquad D_p * \varepsilon_p = 5.\text{E-}13 \text{ m}^2/\text{s}$$

$$K_d = 0.1 \text{ m}^3/\text{kg} \qquad a_L = 50 \qquad \text{m}$$

$$D = 0.05 \text{ m} \qquad b = 5 \cdot 10^{-5} \text{ m}$$

results for he nuclide 237-Np. The normalized flow at the observation point (ℓ = 500 m) is plotted as a function of time for various step sizes along the fracture

$$dz = 25 \quad m \quad dz = 20 \quad m$$

$$dz = 16.\overline{6} \ m \quad dz = 12.5 \ m$$

The discretization in the matrix has been fixed to dr =0.01 m and the order of approximation is 3. As it is seen, the concentration profile is essentially the same for the different step sizes dz besides some deviations in the trailing and leading parts, which are caused not only by the different mesh sizes, but also by the accuracy required for the solution of the differential equation. The maximum concentration deviates less than 1% for dz = 25 m and dz = 12.5 m.

For the same case as before we show the influence of different mesh sizes dr in fig. A.2 for

$$dr = 0.01 \quad m \qquad dr = 0.003\overline{3} \quad m$$

$$dr = 0.005 \quad m$$

with fixed dz = 20 m. Again the results agree within the drawing accuracy . Thus it may be concluded that convergence to a numerical stable solution has been reached for the parameter variation at hand.

For the kakirite case we show in fig. A.3 calculations for the par eters:

$$v_f = 6.03 \quad m/yr \qquad D_p * \varepsilon_p = 5.E{-}13 \ m^2 /s$$

$$K_d = 0.1 \quad m^3 /kg \qquad a_L \quad = 50 \qquad m$$

$$D = 0.055 \text{ m} \qquad R = 5 \cdot 10^{-3} \text{ m}$$

The mesh sizes chosen are

$$dz = 25 \text{ m} \qquad dz = 16.\overline{6} \text{ m}$$

$$dz = 20 \text{ m} \qquad dz = 12.5 \text{ m}$$

and the results show that such spacings in z direction are safe within a few percent deviation.

The dependence of the concentration from the discretization in the matrix is shown in fig. A.4 for:

$$\left. \begin{array}{l} dr = 0.01 \text{ m} \\ dr = 0.005 \text{ m} \\ dr = 0.00\overline{3} \text{ m} \\ dr = 0.0025 \text{ m} \end{array} \right\} \text{order: 2} \qquad \left. \begin{array}{l} dr = 0.01 \text{ m} \\ dr = 0.005 \text{ m} \\ dr = 0.003 \text{ m} \end{array} \right\} \text{order: 4}$$

with fixed dz = 20 m. Compared to the fractured case larger spreading of the results in the leading part of the concentration profile and also in the maximum concentration is obvious. This is caused not only by the additional term $(1/r)(\partial c_p^i/\partial r)$ but also due to the fact that the gradient into the matrix is about two orders of magnitude lower than in the fractured case. Thus, for too large mesh sizes the sharp front of the concentration profile near the interface of the tube and the matrix is badly approximated: numerical dispersion effects show up and, therefore, a finer discretization has to be used.

This effect is demonstrated in fig. A.5 where results are shown for an increased value of $D_p * \varepsilon_p = 5.E-12$ for

$$dr = 0.01 \quad m$$
$$dr = 0.005 \quad m$$
$$\left.\begin{array}{l} \end{array}\right\} \text{order: 2}$$
$$dr = 0.00\overline{3} \quad m$$
$$dr = 0.0025 \quad m$$

$$dr = 0.01 \quad m$$
$$dr = 0.005 \ m$$
$$\left.\begin{array}{l} \end{array}\right\} \text{order: 4}$$
$$dr = 0.00\overline{3} \ m$$

with fixed dz = 20 m. Here, the gradient is a factor of 10 higher and as a consequence step sizes in the matrix are not so critical.

As an other example for the sensitivity of the results with regard to the discretization in the matrix we show in fig. A.6 calculations for the parameters

$$D_p \cdot \varepsilon_p = 5 \cdot 10^{-13} \ m^2/s \qquad K_d = 1 \ m^3/kg$$

and mesh sizes

$$dr = 0.01 \quad m$$
$$dr = 0.005 \quad m$$
$$\left.\begin{array}{l} \end{array}\right\} \text{order: 2}$$
$$dr = 0.00\overline{3} \quad m$$
$$dr = 0.0025 \quad m$$

$$dr = 0.01 \quad m$$
$$dr = 0.005 \ m$$
$$\left.\begin{array}{l} \end{array}\right\} \text{order: 4}$$
$$dr = 0.00\overline{3} \ m$$

Compared to fig. A.4 the spreading of the concentration profile is much more pronounced due to the fact that the sorption capacity of the matrix is a factor of 10 higher.

Based on various other convergence tests we have performed most of the Gewaehr calculations /6/ with fixed spacing dz = 20 m along the fracture/tube. Within the matrix a total of 24 discretization points has been used with variable spacing, being small at the interface tube/matrix and increasing with distance from the ʿʿate

conducting zone.

The accuracy of the results for the Gewaehr calculations may be varying within few percents for cases where the maximum concentration is in the order of 10^{-10} mol/l. For cases where the maximum concentration is in the order of 10^{-20} mol/l results may be accurate up to a factor of 10.
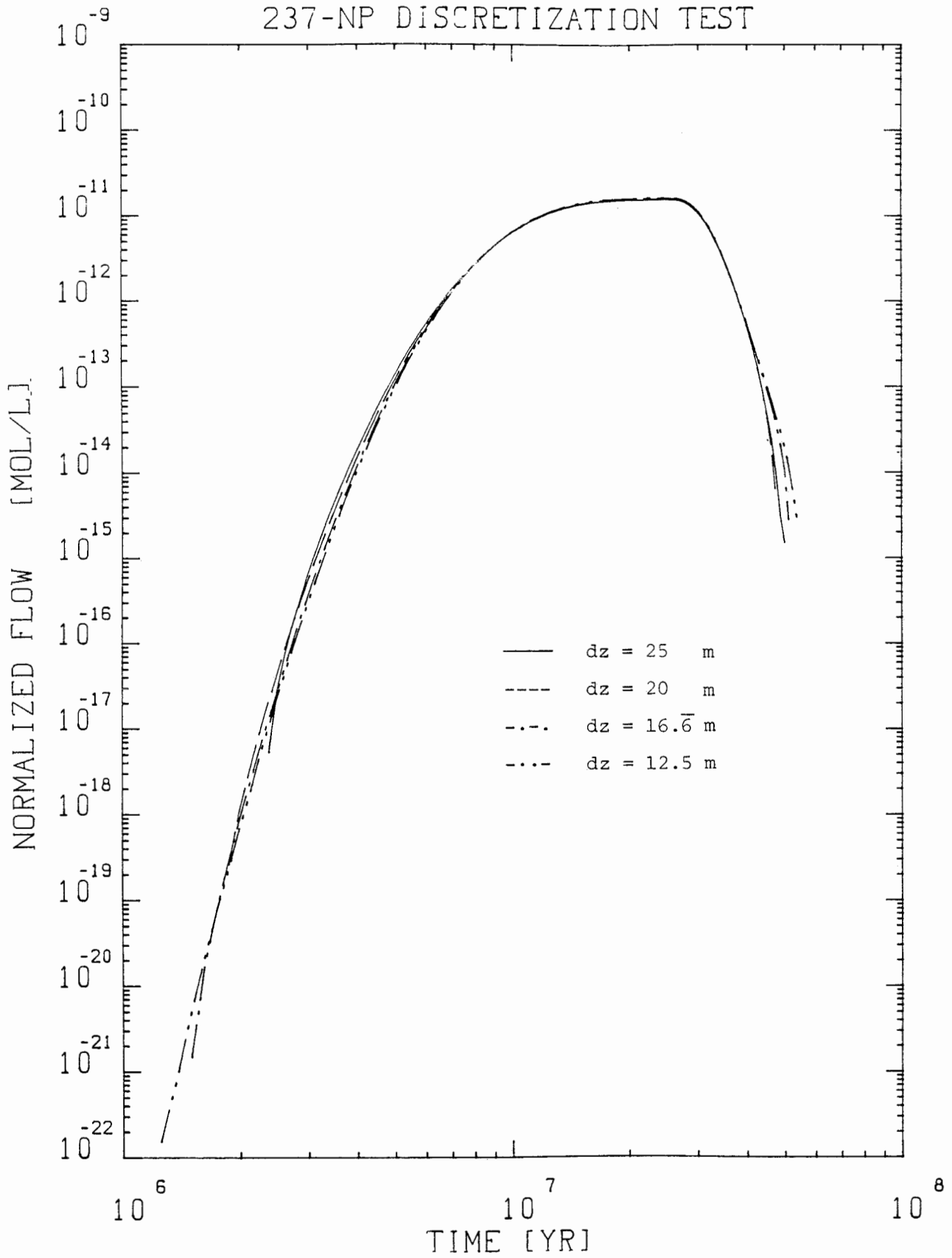
Figure A.1   Normalized flow as a function of time for various mesh sizes
dz as indicated in the figure. dr = 0.01 m and the order of
approximation is 2.
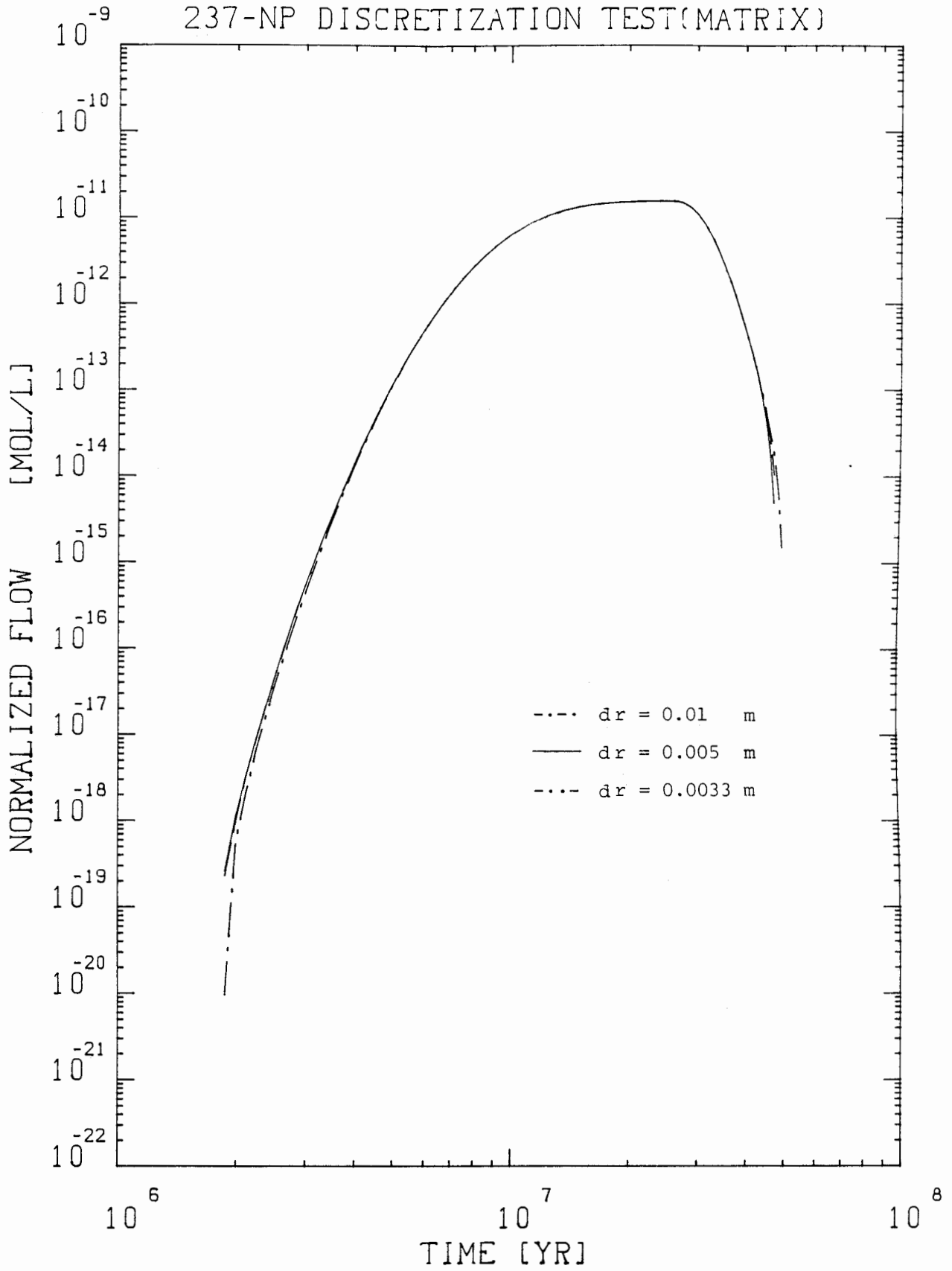
Figure A.2   Normalized flow as a function of time for various mesh sizes
             dr as indicated in the figure. dz = 20 m and the order of
             approximation is 2.
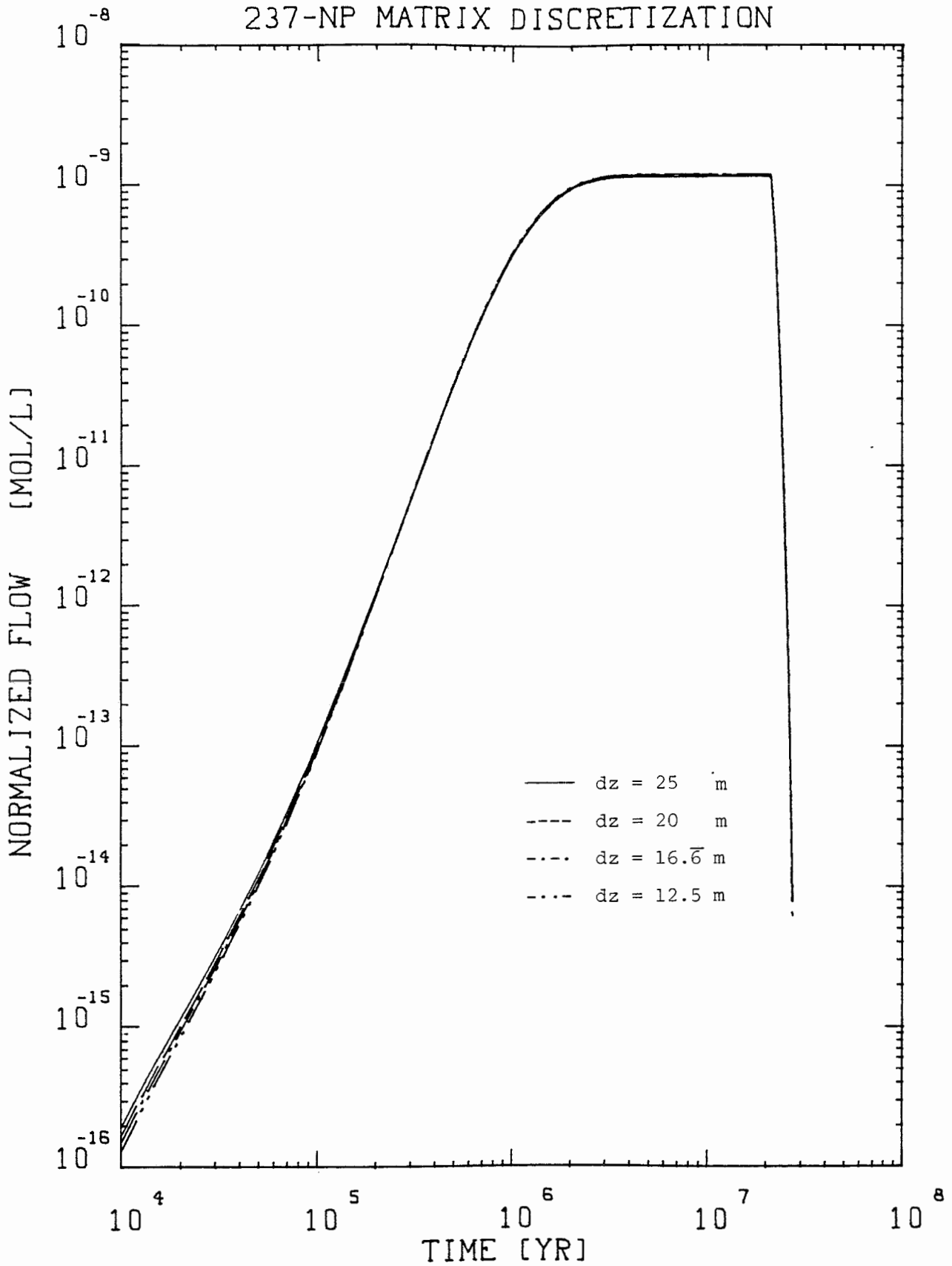
Figure A.3   Normalized flow as a function of time for various mesh sizes
dz as indicated in the figure. dr = 0.005 m and the order of
approximation is 2.
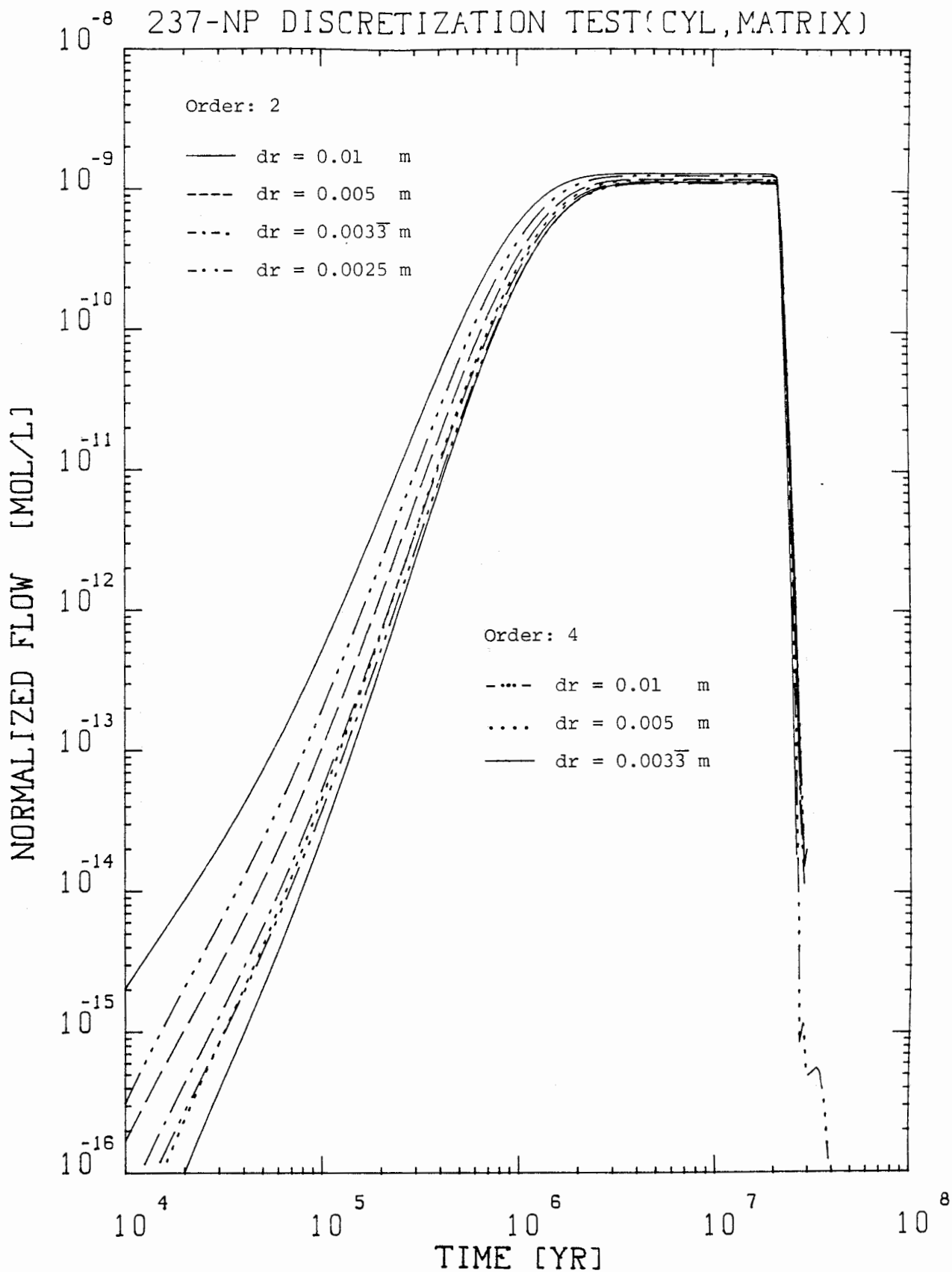
Figure A.4   Normalized flow as a function of time for various mesh sizes
dr and different orders of approximations as indicated in the
figure. d z = 20 m.
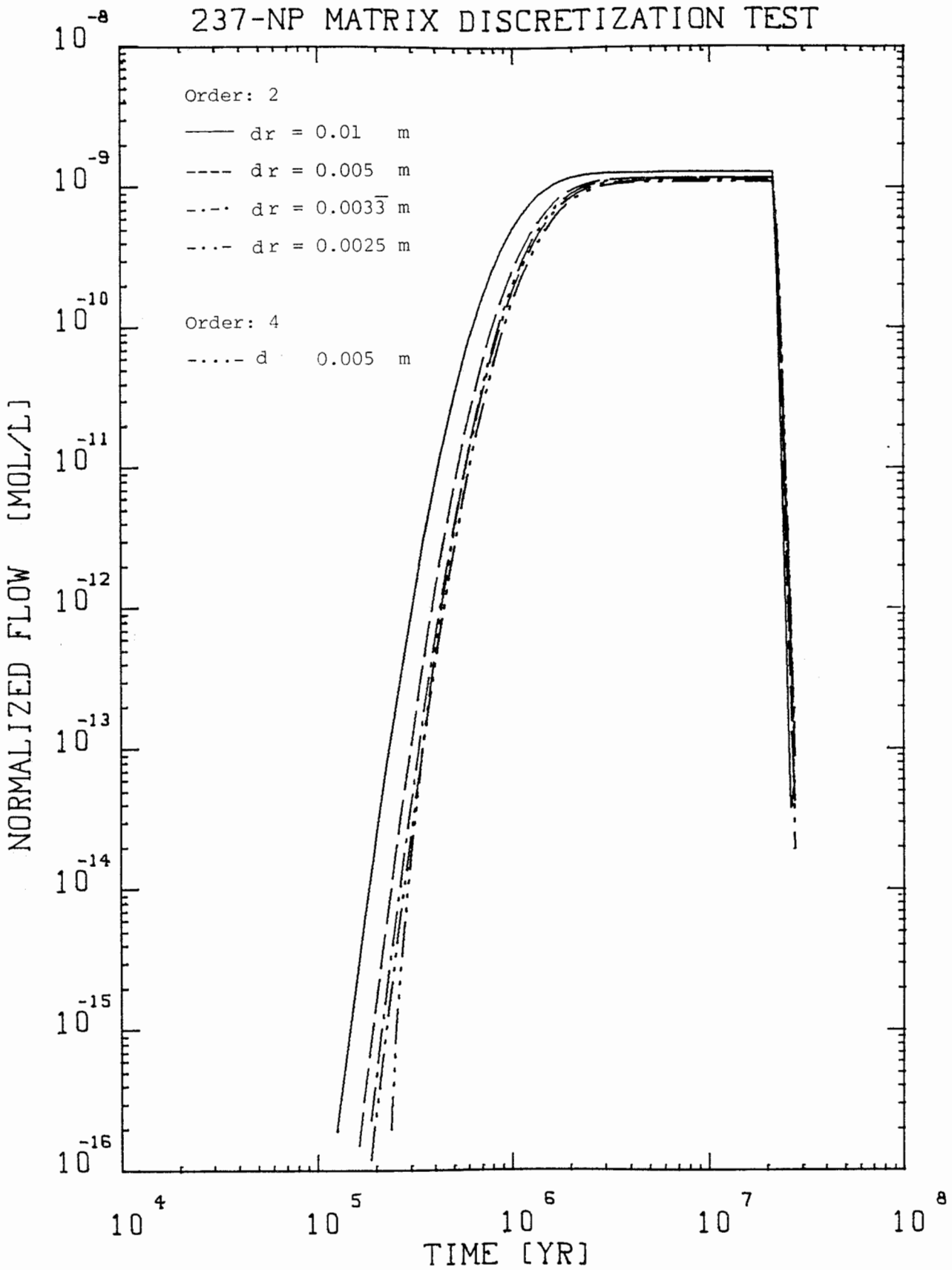
Figure A.5 Normalized flow as a function of time for various mesh sizes dr and different orders of approximation as indicated in the figure.
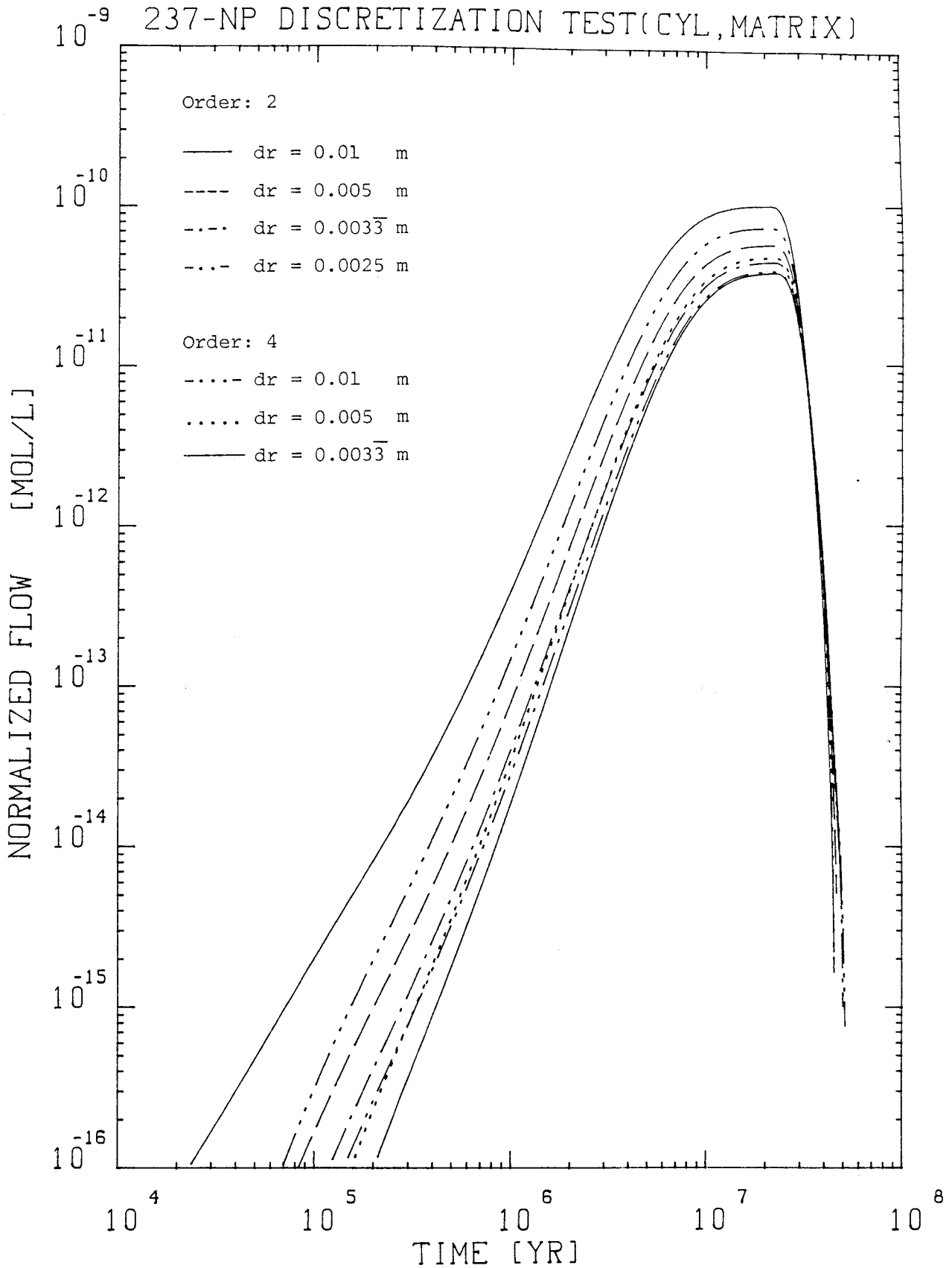
Figure A.6   Normalized flow as a function of time for various mesh sizes
             dr and different orders of approximations as indicated in the
             figure.

REFERENCES

/1/ NAGRA, "Projekt Gewaehr 1985, Endlager fuer hochaktive Abfaelle: Das System der Sicherheitsbarrieren", Projektbericht NGB 85-04, Baden 1985

/2/ NAGRA, "Sondierbohrung Boettstein - Untersuchungsbericht", NAGRA NTB 85-01, Baden 1985, and Tj. Peters, private communication, Oct., 29, 1984

/3/ G.E. Grisak and J.F. Pickens, Water Res. Res. 16 (1980)719

/4/ I. Neretnieks, J. Geophys. Res. 85 (1980)4379

/5/ N.A. Chapman and I.G. McKinley, "The Potential of Natural Analogues in Assessing Systems for Deep Disposal of High-Level Radioactive Waste", NAGRA NTB 84-41, Baden 1985, and EIR-Bericht Nr. 545, Wuerenlingen 1985

/6/ NAGRA, "Projekt Gewaehr 1985, Endlager fuer hochaktive Abfaelle: Sicherheitsbericht", Projektbericht NGB 85-05, Baden 1985

/7/ J. Bear, Hydraulics of Groundwater, McGraw-Hill, New York 1979

/8/ A. Avogadro, G. de Marsily, "The Role of Colloids in Nuclear Waste Disposal" in Sci. Basis for Nuclear Waste Management VII (G.L. McVay, ed.), North-Holland, New York 1984

/9/ J. Hadermann, Nucl. Technol. 56 (1982)102

/10/ E. Ledoux, G. de Marsily, "First attempt to evaluate the transport of colloids in a fracture with redisolution and diffusion of the solute in the matrix", Ecole des Mines de Paris 1984

/11/ I.G. McKinley and J. Hadermann, "Radionuclide Sorption Database for Swiss Safety Assessments", NAGRA NTB 84-40, Baden 1985, and EIR-Bericht Nr. 550, Wuerenlingen 1985

/12/ J. Hadermann and F. Roesel, "Numerical Solution of the Radionuclide Transport Equation; Non-Linear Sorption Effects", NAGRA NTB 83-23, Baden 1983, and EIR-Bericht Nr. 506, Wuerenlingen 1983

/13/ U. Schmocker, Der Einfluss der transversalen Diffusion/Dispersion auf die Migration von Radionukliden in poroesen Medien - Untersuchung analytisch loesbarer Probleme fuer geologische Schichtstrukturen, NAGRA NTB 80-06, Baden 1980, and EIR-Bericht Nr. 405, Wuerenlingen 1980

/14/ A. Larsson, K. Andersson, B. Grundfelt, J. Hadermann, "Mathematical Models for Nuclide Transport in Geologic Media: An International Intercomparison (INTRACOIN)", in Radioactive Waste Management, IAEA Vienna 1984, Vol. 5, p. 197

/15/ F. Roesel and J. Hadermann, "Two-Dimensional Benchmark Calculations with Code RANCH2N", EIR internal report, TM-45-83-45, Wuerenlingen 1983

/16/ J. Hadermann and F. Roesel, "INTRACOIN, level 2 case 2a; A one-dimensional approach; EIR internal report, TM-45-83-10, Wuerenlingen 1983

/17/ I. Neretnieks, private communication, Nov. 6., 1984

/18/ E.A. Sudicky and E.O. Frind, Water Res. Res. 18 (1982)1634

/19/ G.E. Grisak and J.F. Pickens, J. Hydrol. 52 (1981)47

/20/ A. Rasmuson and I. Neretnieks, AIChE Journal 26 (1980)686

/21/ J. Hadermann, "Radionuklidtransport durch Risssysteme · und Matrixdiffusion", EIR internal report, TM-45-81-42, Wuerenlingen 1981

/22/ J. Hadermann and F. Roesel, "Matrix diffusion", EIR internal report, TM-45-84-26, Wuerenlingen 1984

/23/ R. Hartley, "Release of radionuclides to the geosphere from a repository for high-level waste - Mathematical model results", NAGRA NTB 85-41, Baden 1985

/24/ M. Schweingruber, "Actinide and Tc Solubilities in Deep - Crystalline Reference Groundwater Defined for NAGRA Project "Gewaehr"", EIR internal report, TM-45-84-30, Wuerenlingen 1984

/25/ J.M. Hyman, Method of lines Solution of Partial Differential Equations, Courant Institute of Mathematical Science, C00-3077-139 (1976)

/26/ See for example : J. Collatz, The numerical Treatment of Differential Equations, Springer, Berlin 1960

/27/ G.W. Gear, The Automatic Integration of Ordinary Differential Equations, Comm. ACM, 14 (1971)176

/28/ IMSL - Library, Edition 9 (1982)

/29/ S.C. Eisenstat, M.C. Gursky, M.H. Schultz and A.H. Sherman, Yale Sparse Matrix Package Research Report 114

/30/ F. Roesel and J. Hadermann, Description of the Computer Code RANCHMD, EIR internal report to be published (1985)

/31/ INTRACOIN, "International nuclide transport code intercomparison study, Draft final report levels 2 and 3", Stockholm 1984

/32/ F. Roesel and J. Hadermann, INTRACOIN LEVEL 3, Fractured Media Case Calculations, EIR internal report, TM-45-84-29, Wuerenlingen 1984

Water flow through the repository Q_L	4.2	m^3/yr
Hydraulic conductivity K	$1.25 \cdot 10^{-9}$	m/s
Hydraulic gradient $\nabla \phi$	0.012	m/m
Tube frequency n' $(=n^2/4D^2)$	* 1 (9)	m^{-2}
Fracture frequency $\bar{n}$	* 10 (1)	m^{-1}
Tube radius R	* $5 \cdot 10^{-3}$ $(5 \cdot 10^{-4})$	m
Fracture half-width b	* $5 \cdot 10^{-5}$	m
Extent of altered zone D		
a) kakirite veins	0.5 (var)	m
b) aplite fractures	$1 \cdot 10^{-3}$ (var)	m
Density of altered zones ρ	2616	kg/m^3
Porosity of altered zone ε_p	0.033	m^3/m^3
Diffusion constant in altered zone D_p	* $1.515 \cdot 10^{-10}$	m^2/s
	$(1.515 \cdot 10^{-11}$	$m^2/s)$
Dispersion length a_L	* 50 (250)	m
Migration distance ℓ	500	m

Table I: Nuclide independent parameters for the geosphere transport calculations. The numbers in parentheses define parameter variations of a base case, var indicating values as given in the text. The parameters values with an asterisk are more or less educated guesses. The others follow from model calculations or experimental measurements within "Projekt Gewaehr 1985" /1/.

Nuclide i	Half-life $\tau_{1/2}$ [yr]	Distribution constant K_d^i [m³/kg]	Solubility limit C_L^i [mol/l]
237-Np	$2.14 \cdot 10^6$	1 (0.1)	$2.0 \ 10^{-9}$
233-U	$1.592 \cdot 10^5$	1 (0.05)	$2.5 \ 10^{-9}$
229-Th	$7.34 \cdot 10^3$	1 (0.01)	$1.6 \ 10^{-8}$

Table II: Nuclide dependent parameters for the geosphere transport calculation. The values for distribution constants are taken from ref. /11/, numbers in parentheses define variations from a base case. The solubility limits are taken from ref. /24/ and given for comparison purposes.
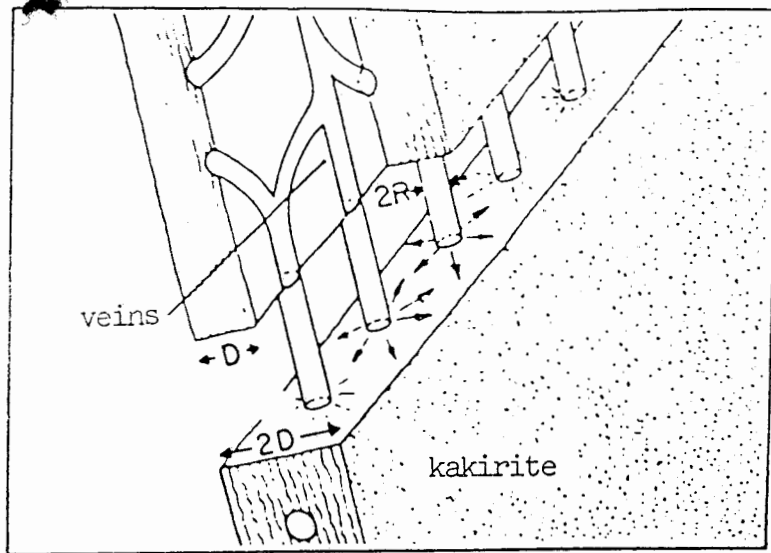
Figure 1a   Schematic model for the transport in kakirite zones.
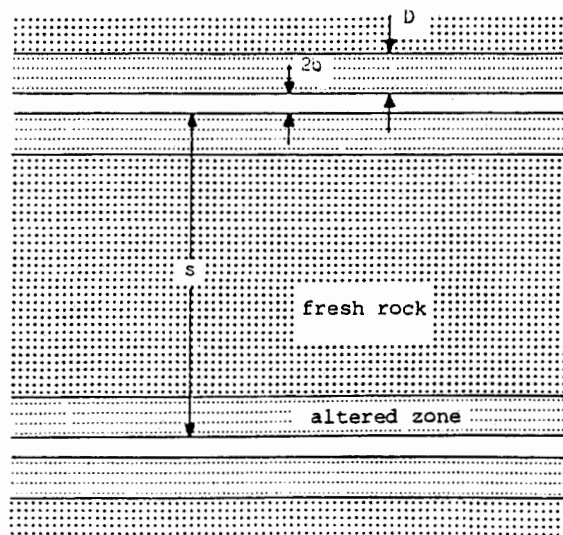
Figure 1b   Schematic model for the transport in fracture zones.
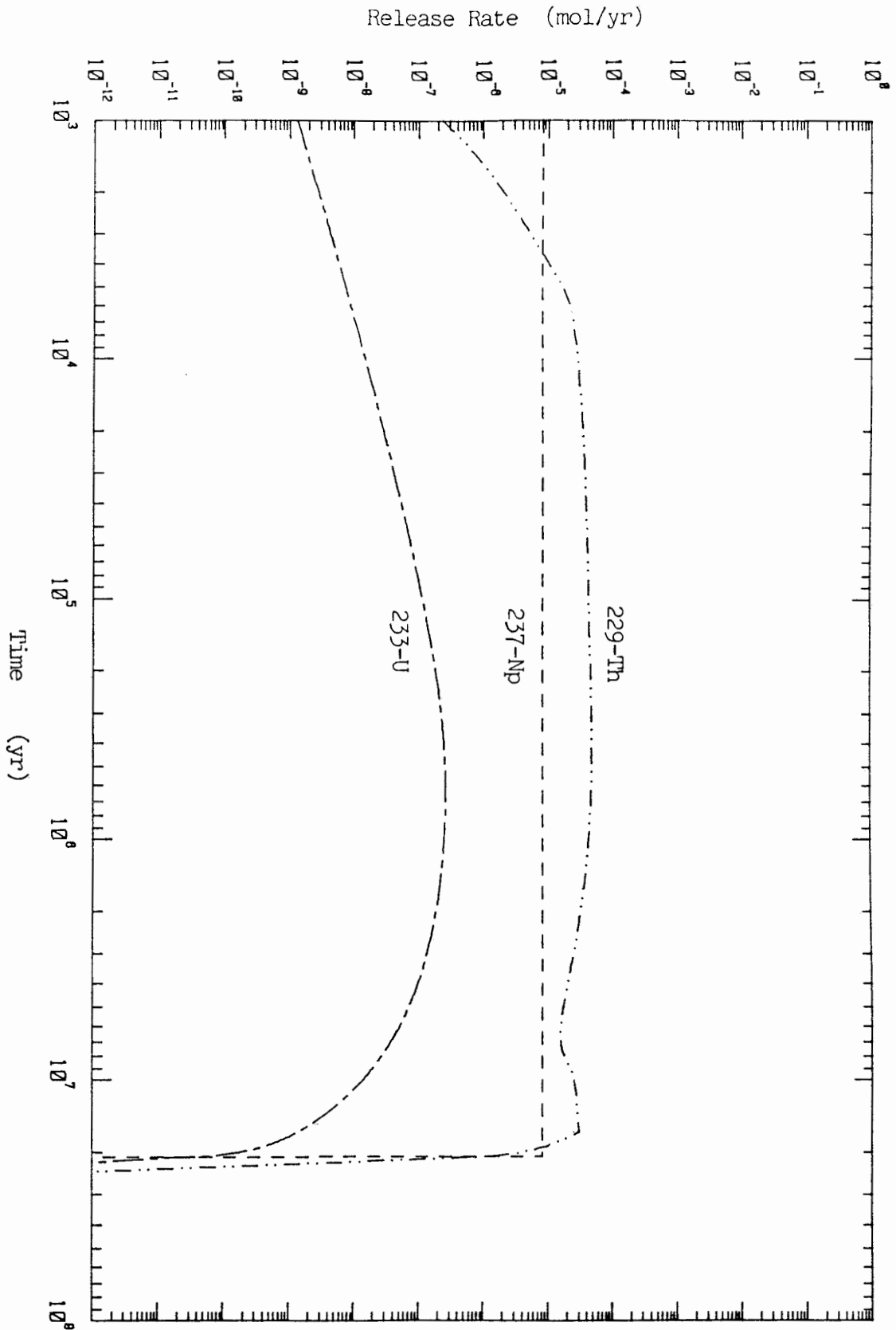
Figure 2   Release rate into the geosphere for the 237-Np chain as a
function of time after emplacement into the repository.
Canister life-time is 1000 years.
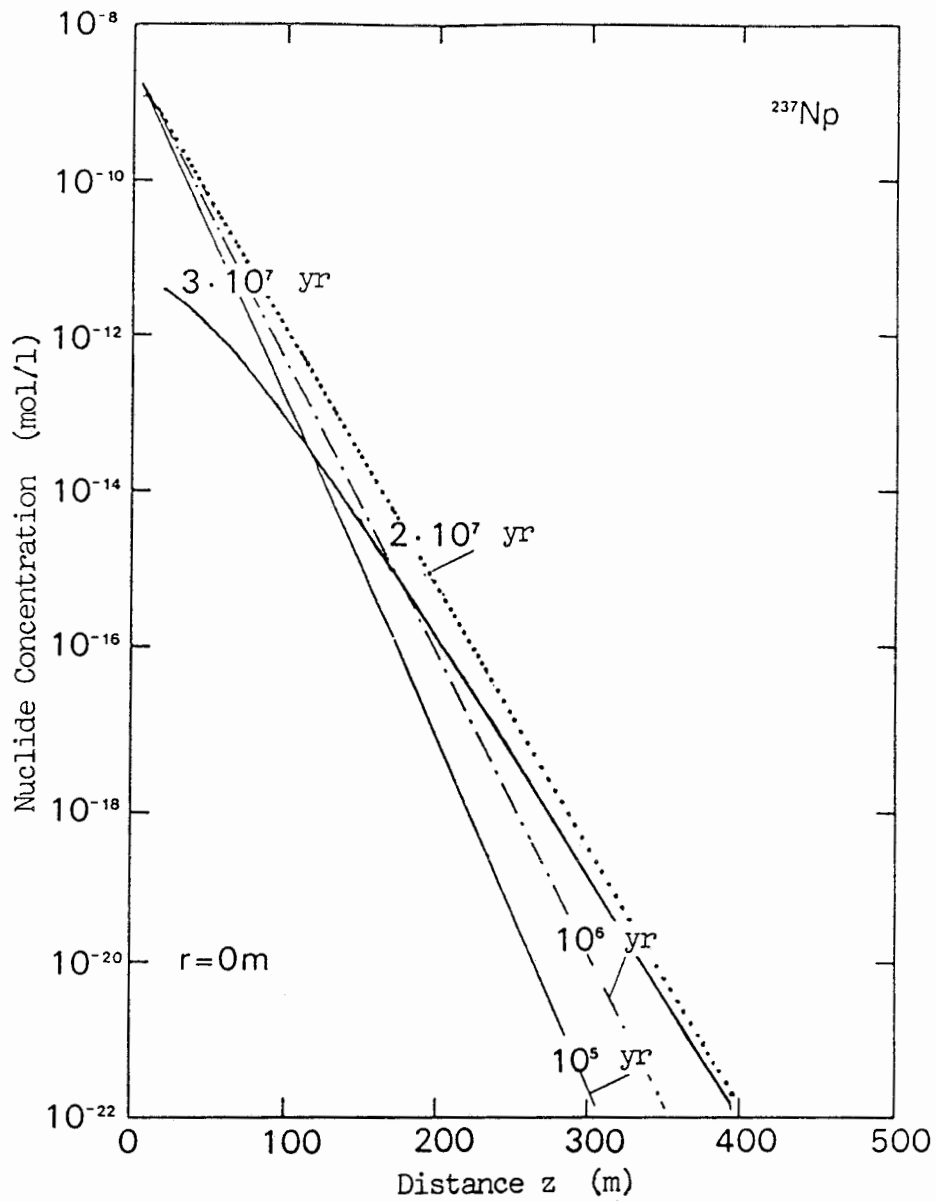
Figure 3   Concentration of 237-Np in the water conducting kakirite veins as a function of distance from the inlet for various times after canister failure. The parameters are those of the base case.
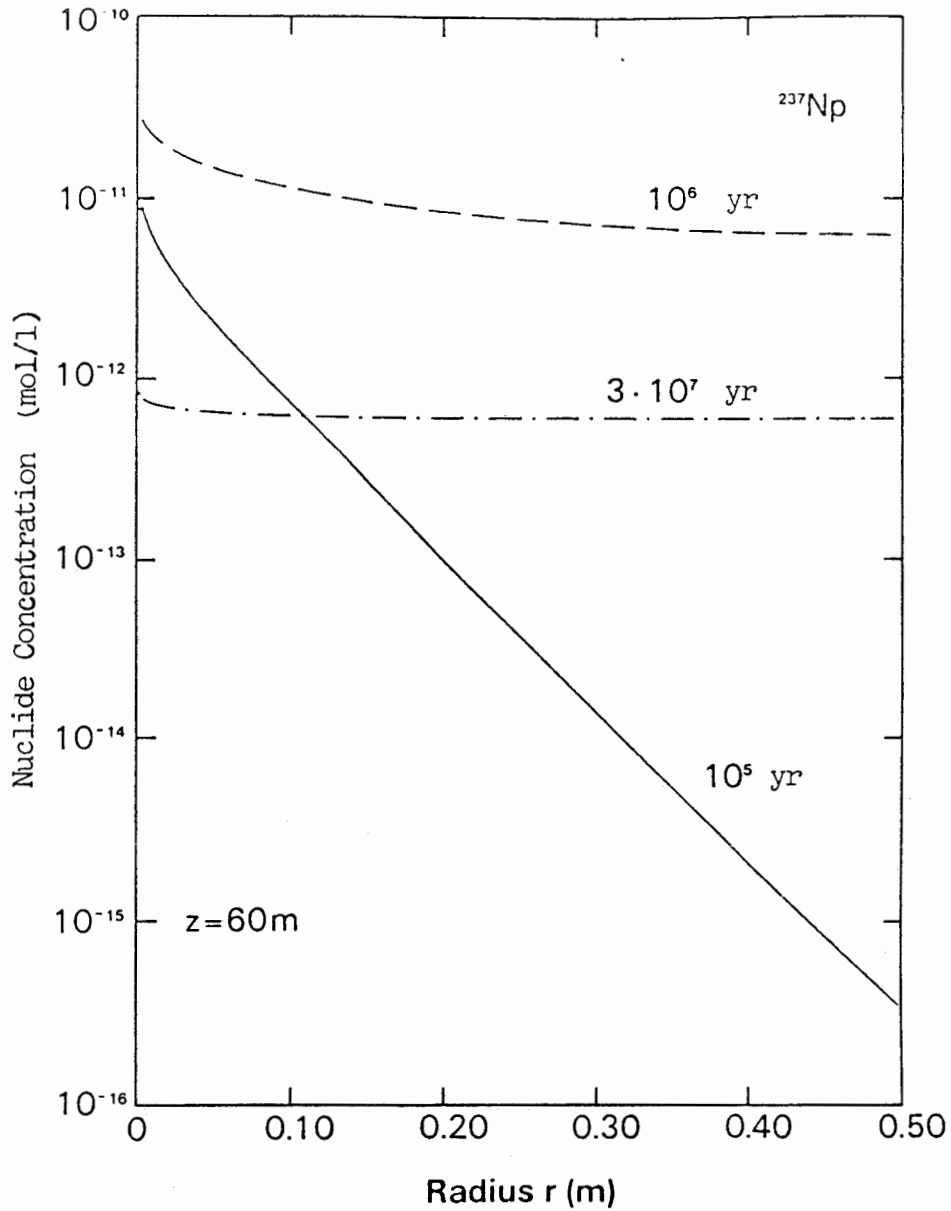
Figure 4   Concentration of 237-Np in the kakirite at a distance of
            60 m from the geosphere inlet as a function of distance
            from the water conducting vein for various times after
            canister failure. The parameters are those of the base
            case.
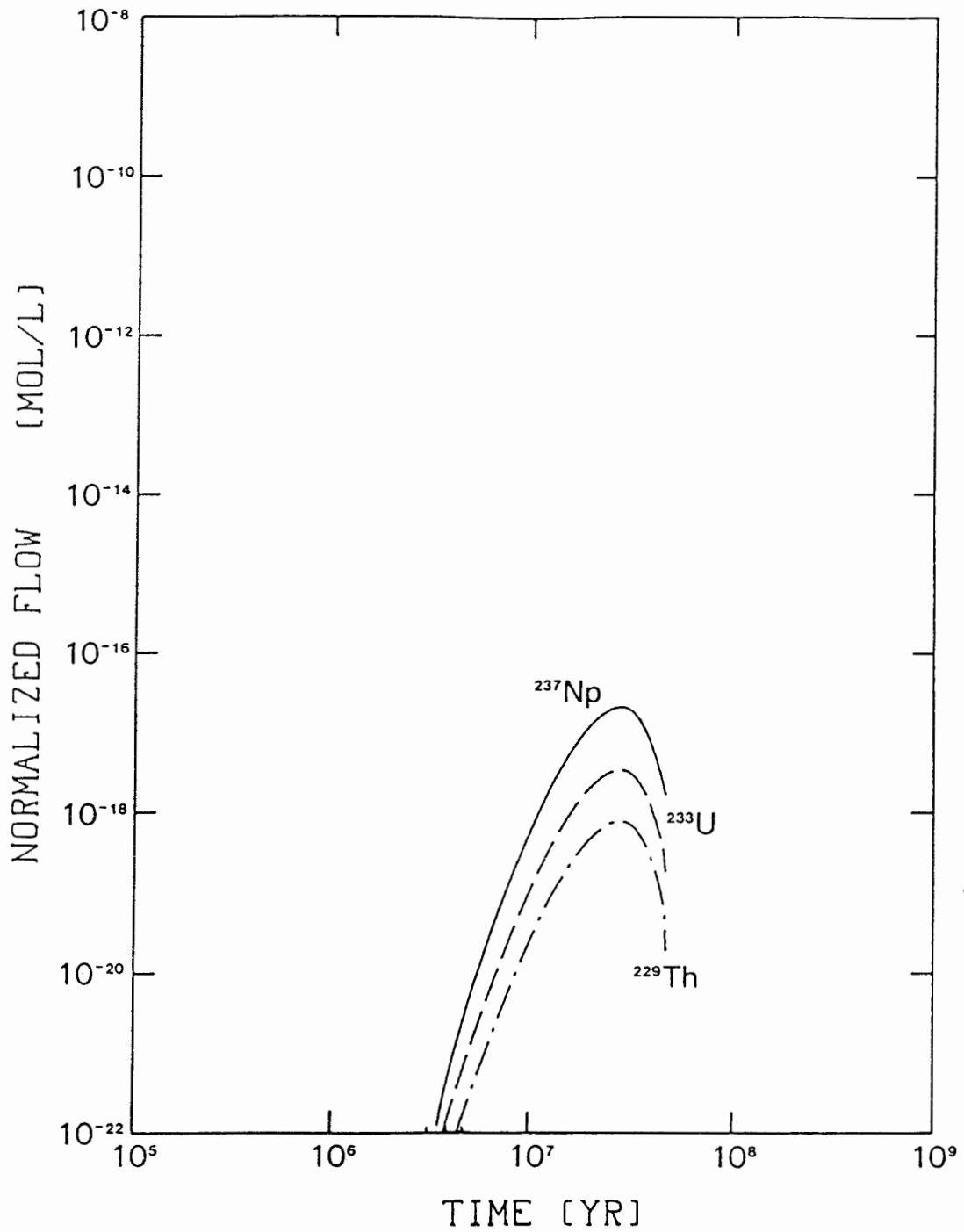
Figure 5   Nuclide flows after a migration distance of 500 m normalized
           to a water flow of 4.2 m^3/yr as a function of time after ca-
           nister failure. Presented are the results for the three mem-
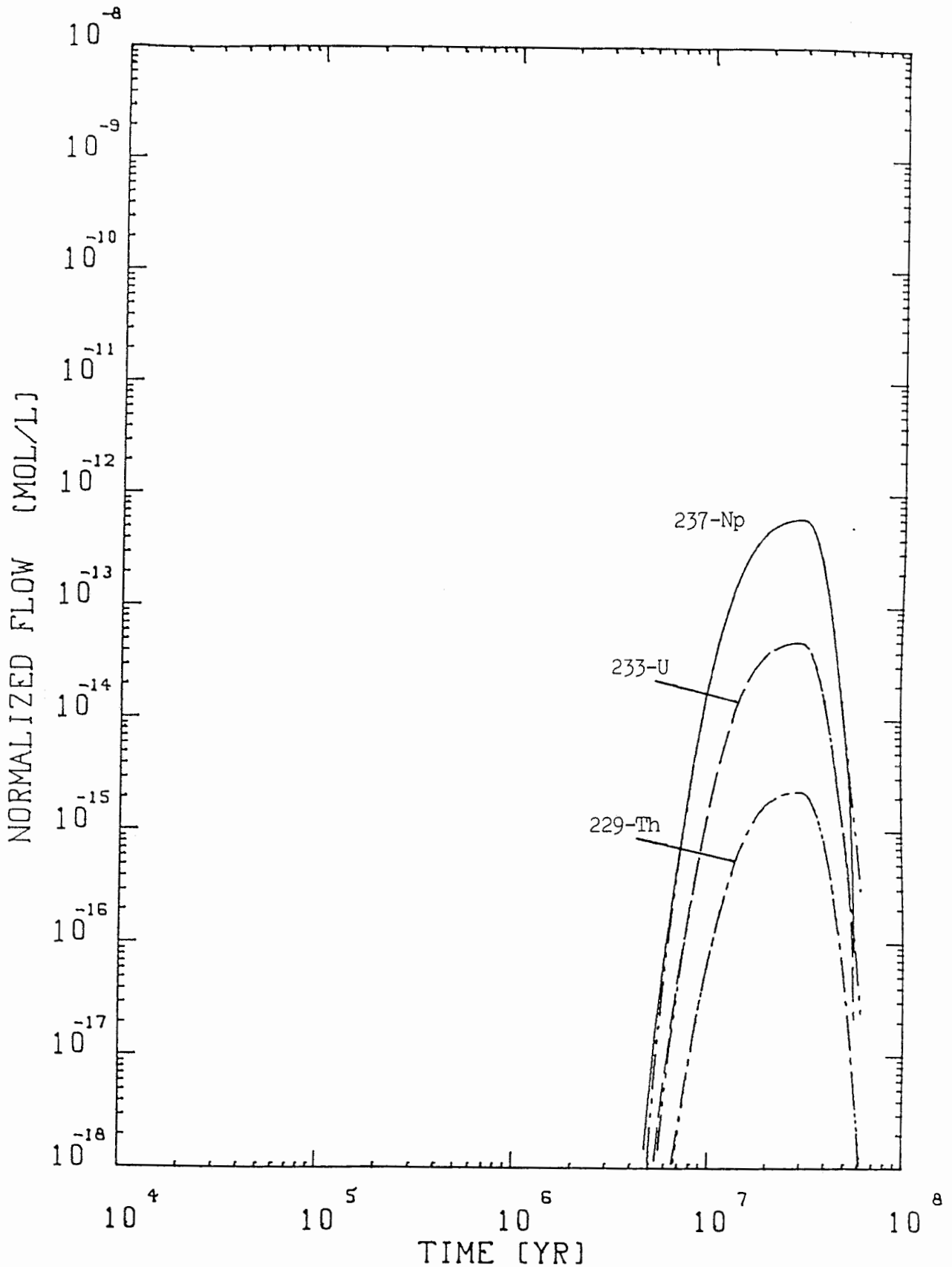   ber chain 237-Np → 233-U → 229-Th for transport in the kaki-
           rite zone. The parameters are those of the base case except
           for the sorption distribution constants (low set).
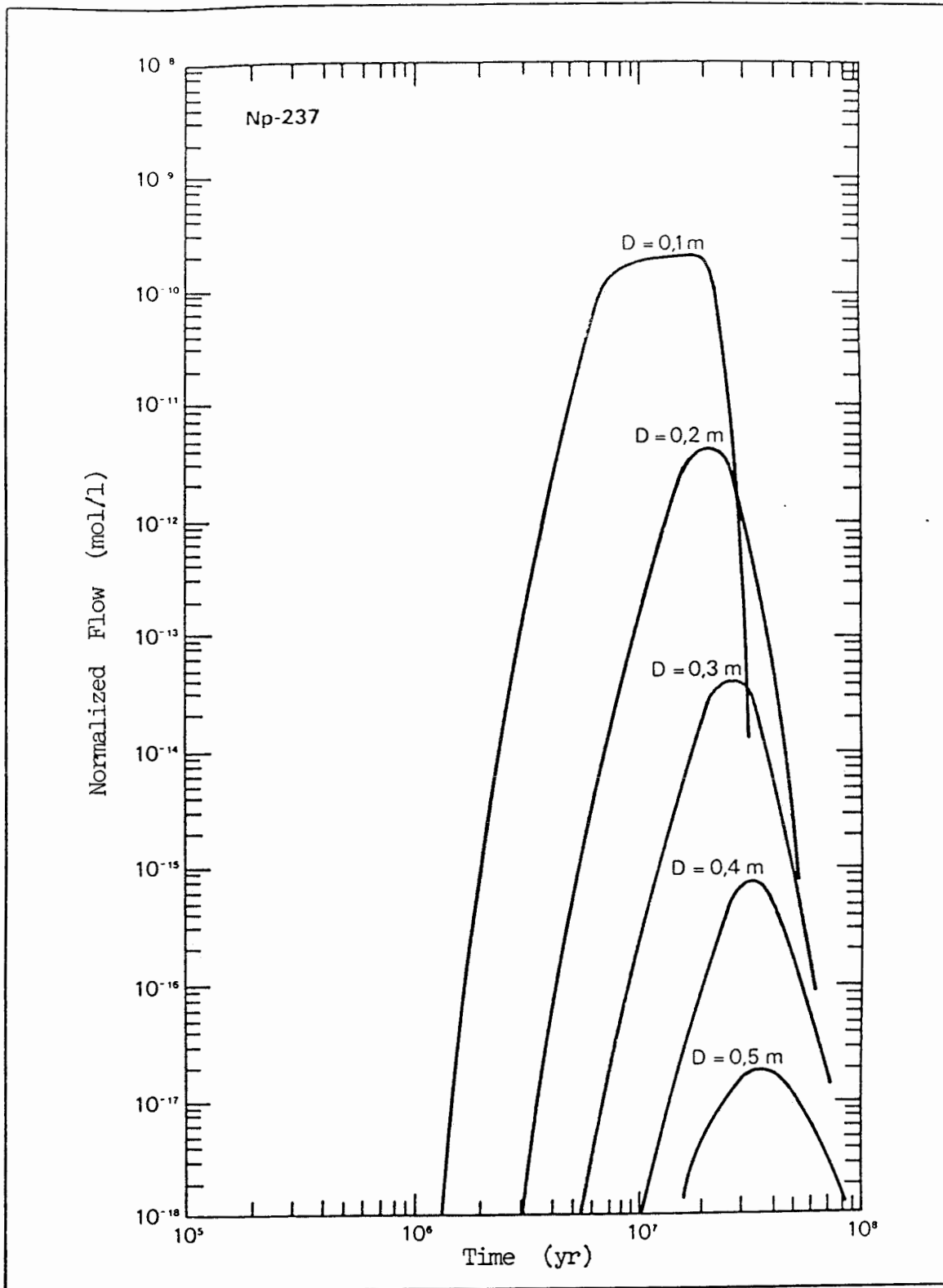
Figure 6   Effect of kakirite width on 237-Np flows after a migration dis-
tance of 500 m. The parameters are those of figure 5 with the
exception of the kakirite width which is indicated in the figure.
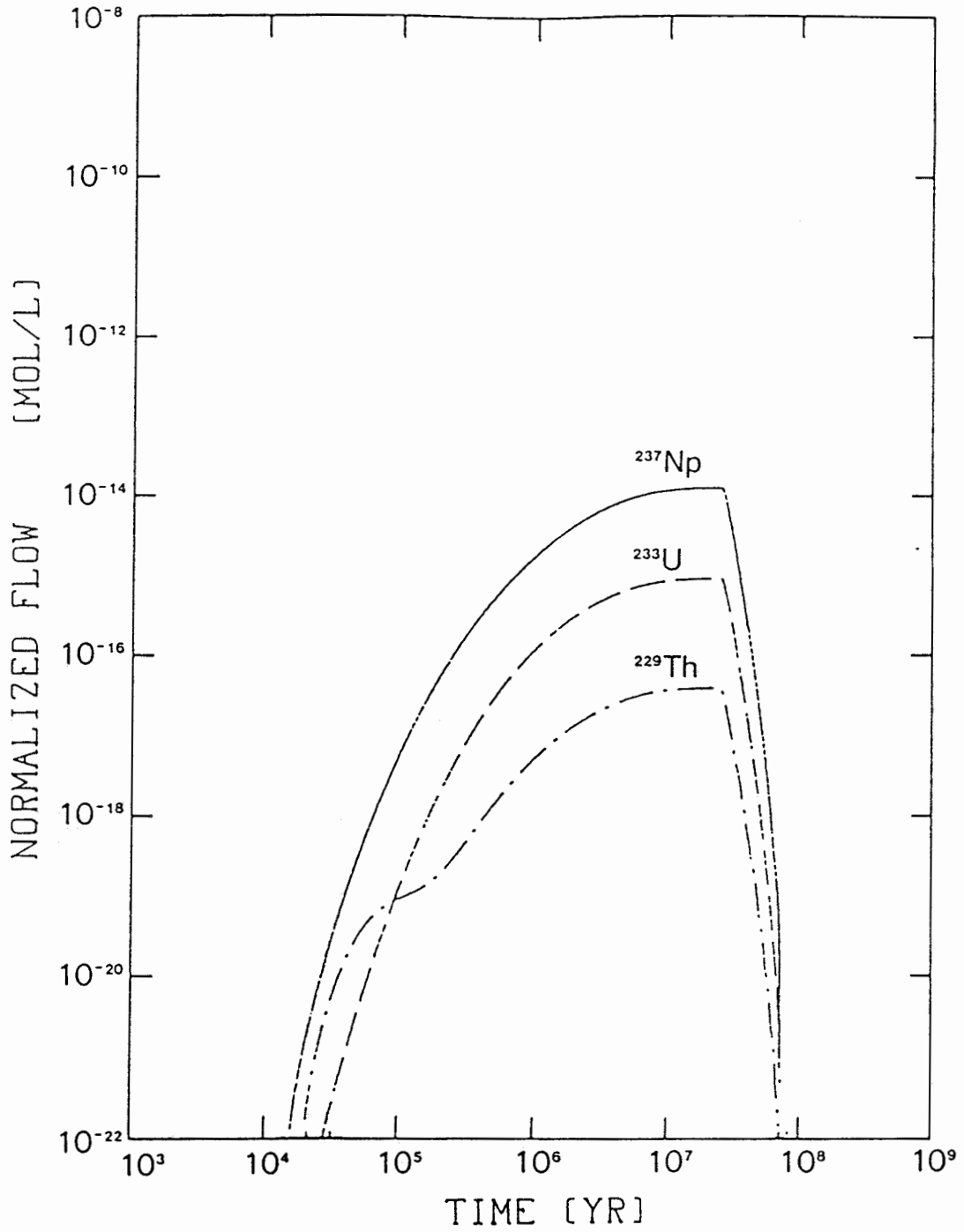
Figure 7   The same as figure 5. The parameters are those of the base
case except for diffusion constant in the kakirite zone
(low value).
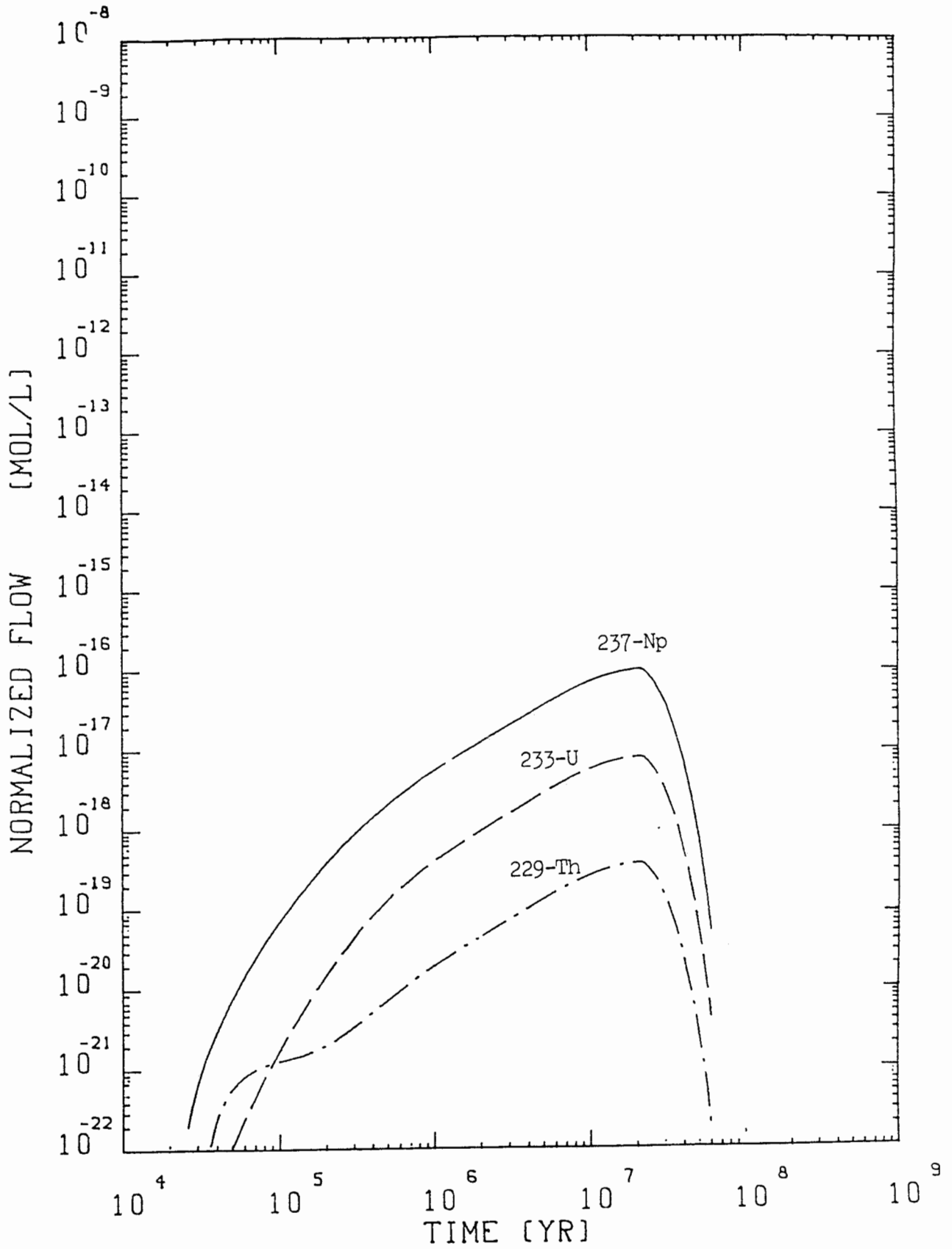
Figure 8   The same as figure 5. The parameters are those of the base
            case with the exception of the longitudinal dispersion
            length (high value).
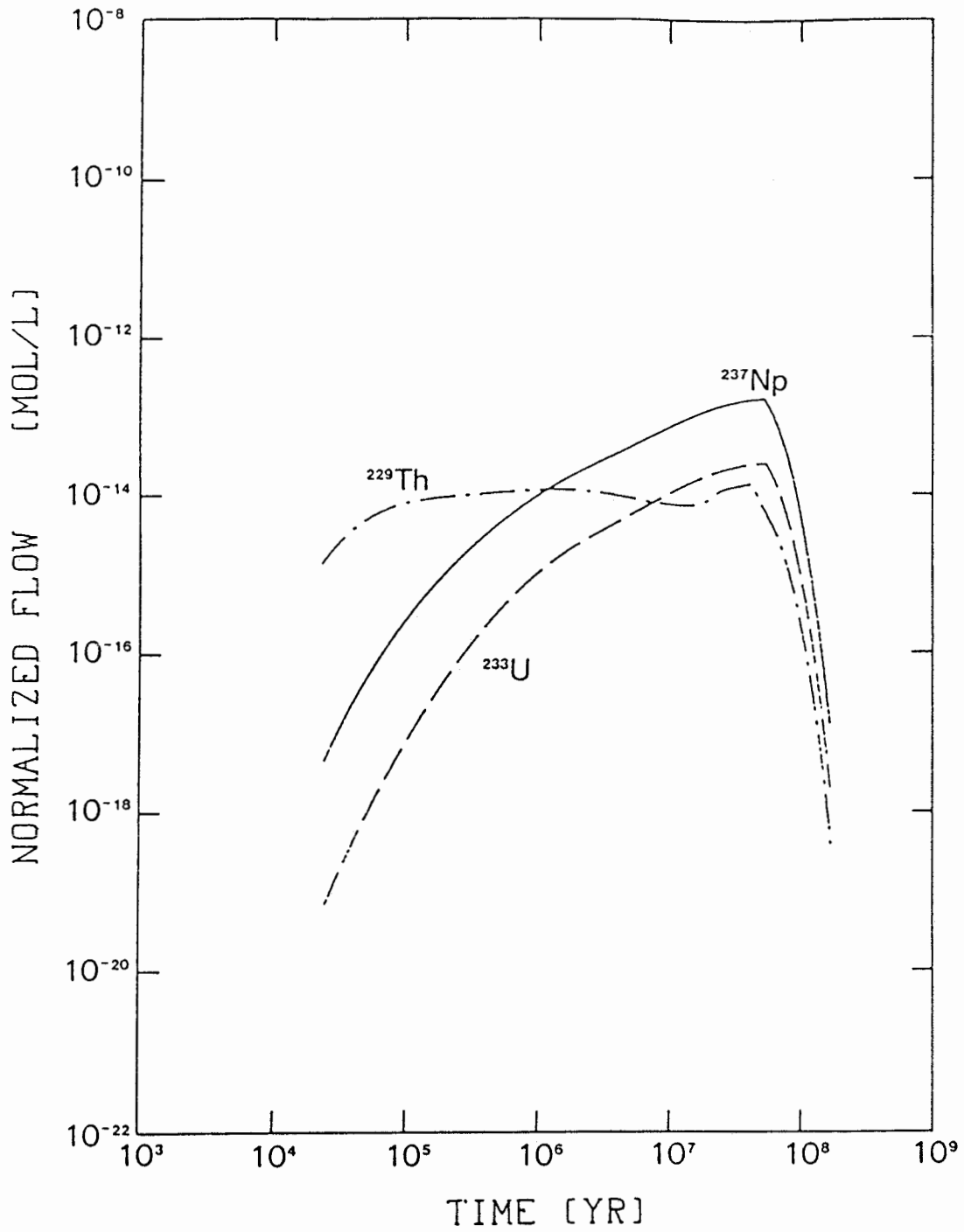
Figure 9   The same as figure 5. The parameters are those of the base
           case with the exception of sorption distribution constants
           (set of low values) and the diffusion constant in the kaki-
           rite zone (low value).

Figure 10   Nuclide flows after a migration distance of 500 m normalized
             to a water flow of 4.2 m³/yr as a function of time after ca-
             nister failure. Presented are the results for the 237-Np chain
             for transport in the fractured aplite-pegmatite dykes. The
             dash-two-dots, dash-three-dots and fully dotted lines are those
             for the effective surface sorption approximation. The parameters
             are those of the base case.
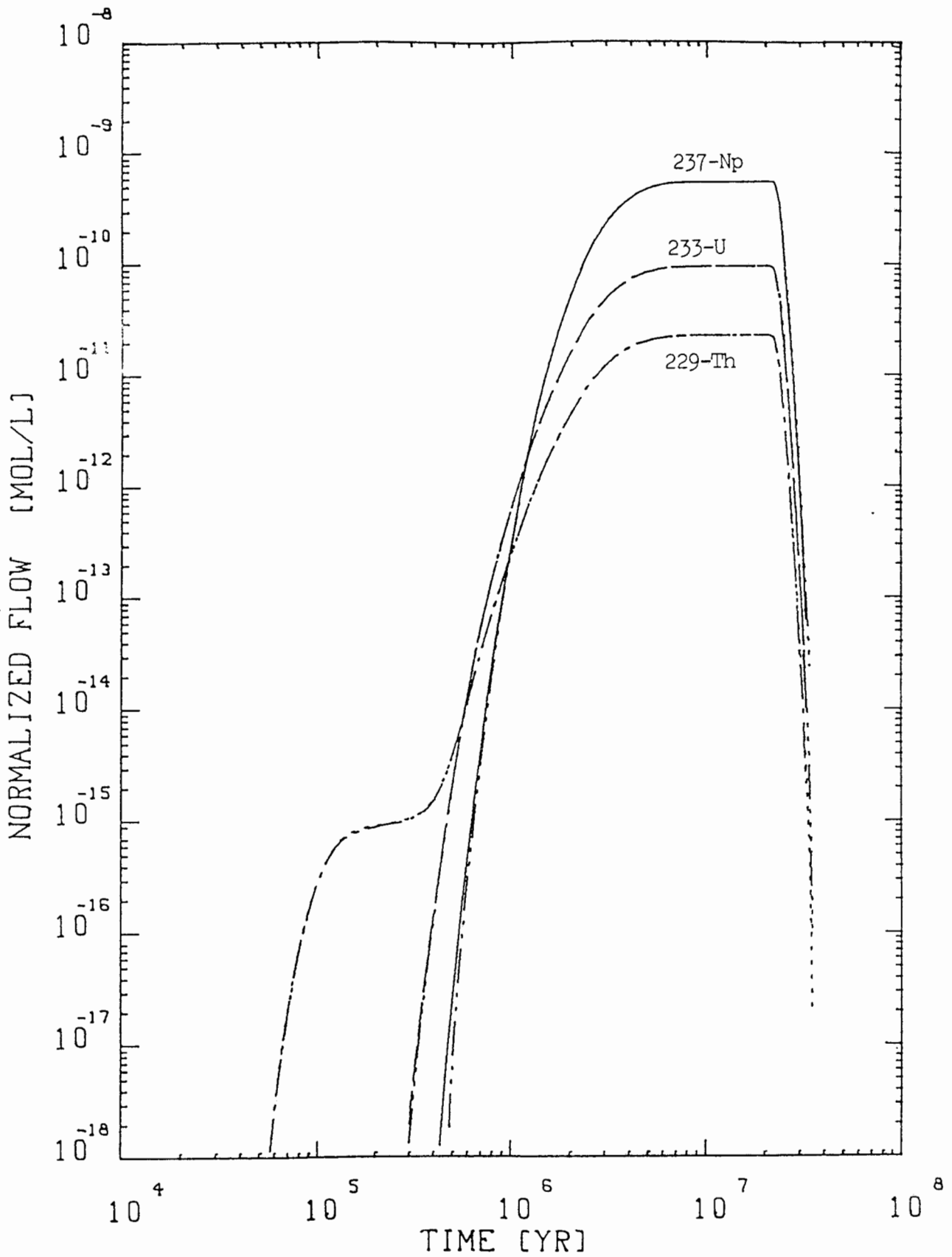
Figure 11 The same as figure 10. The parameters are those of the base case except for the sorption distribution constants (low values set).
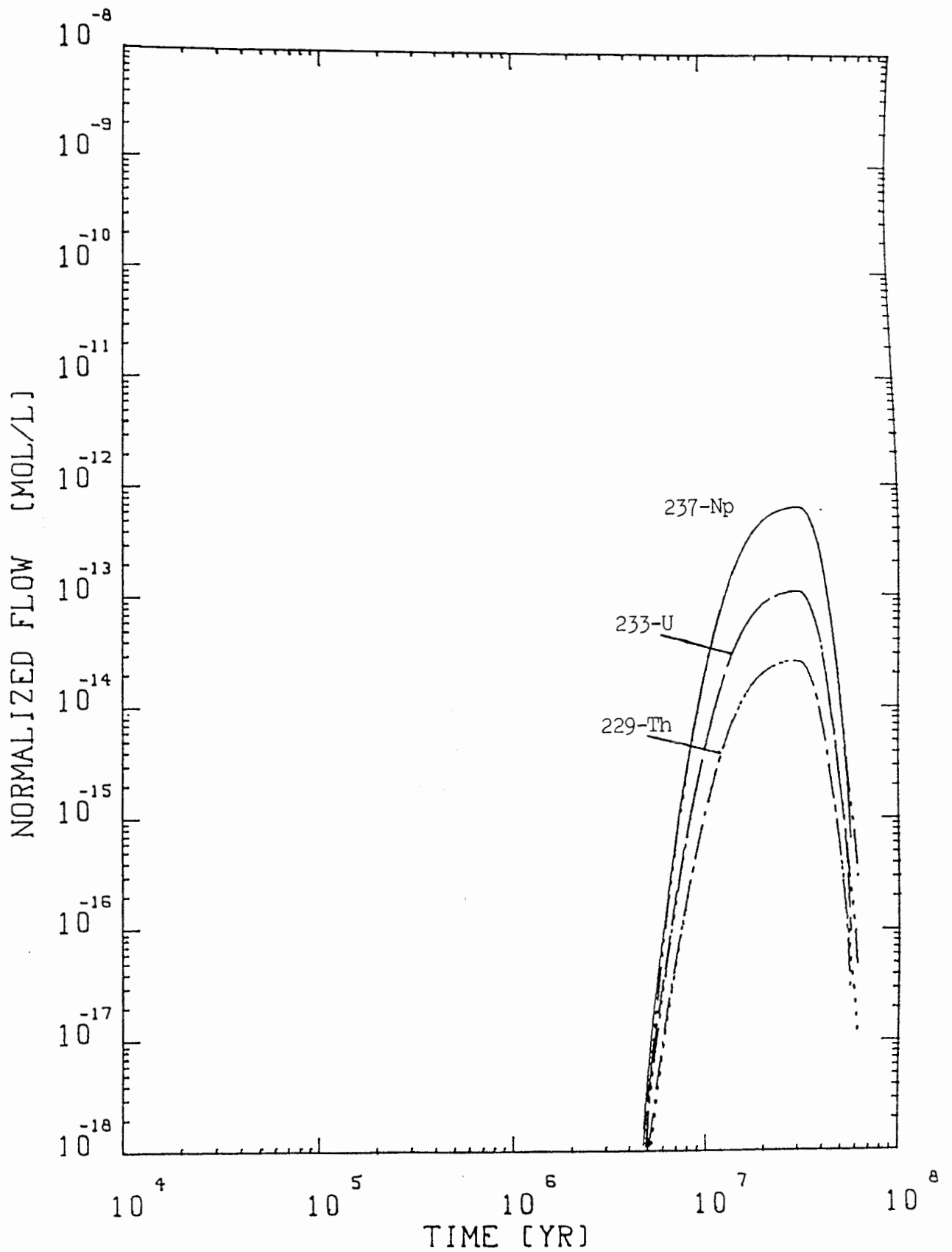
Figure 12   The same as figure 11 but with an increased width of altered
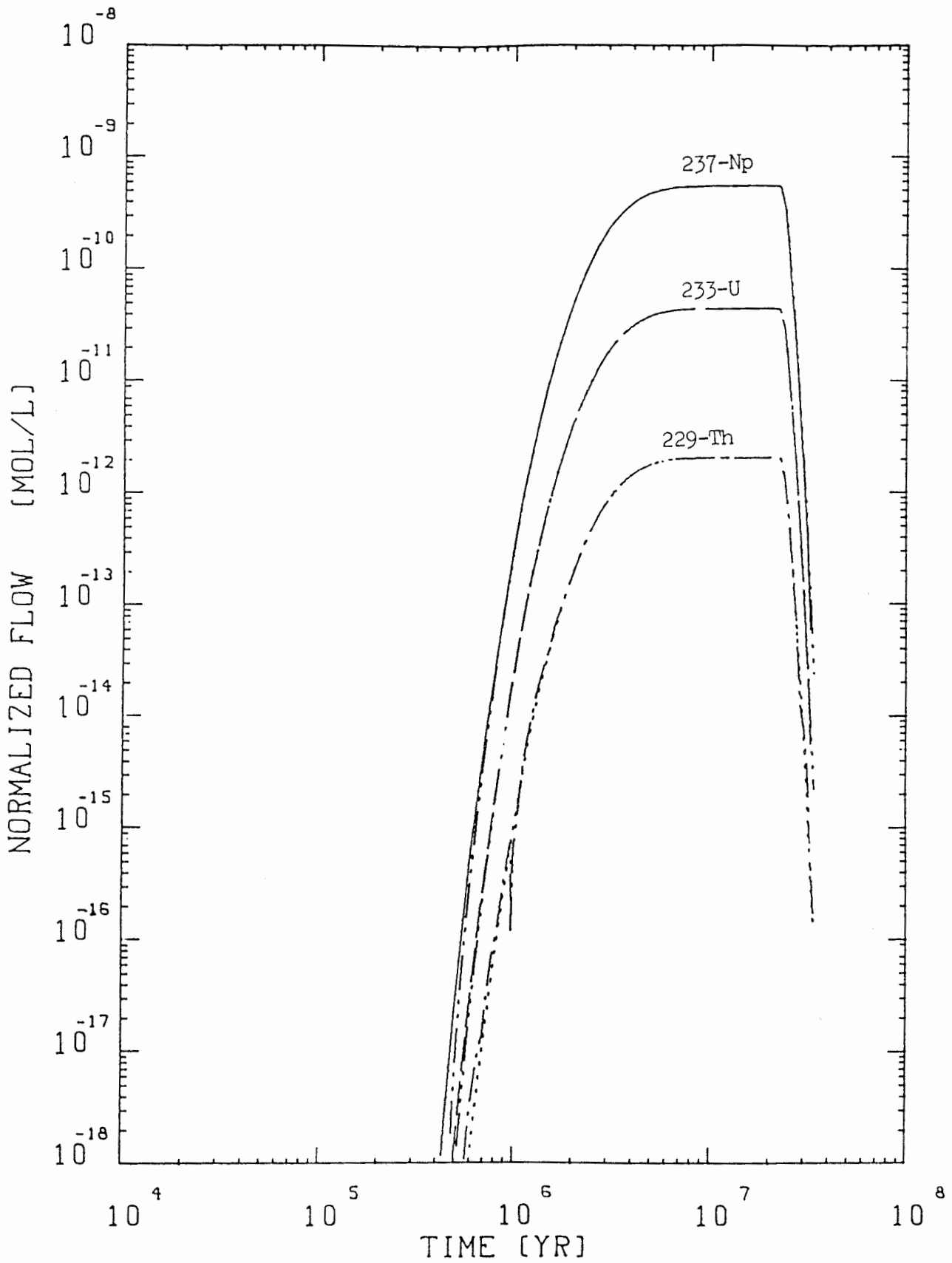   zone (D = 0.01 m).

Figure 13   The same as figure 10. The parameters are those of the base
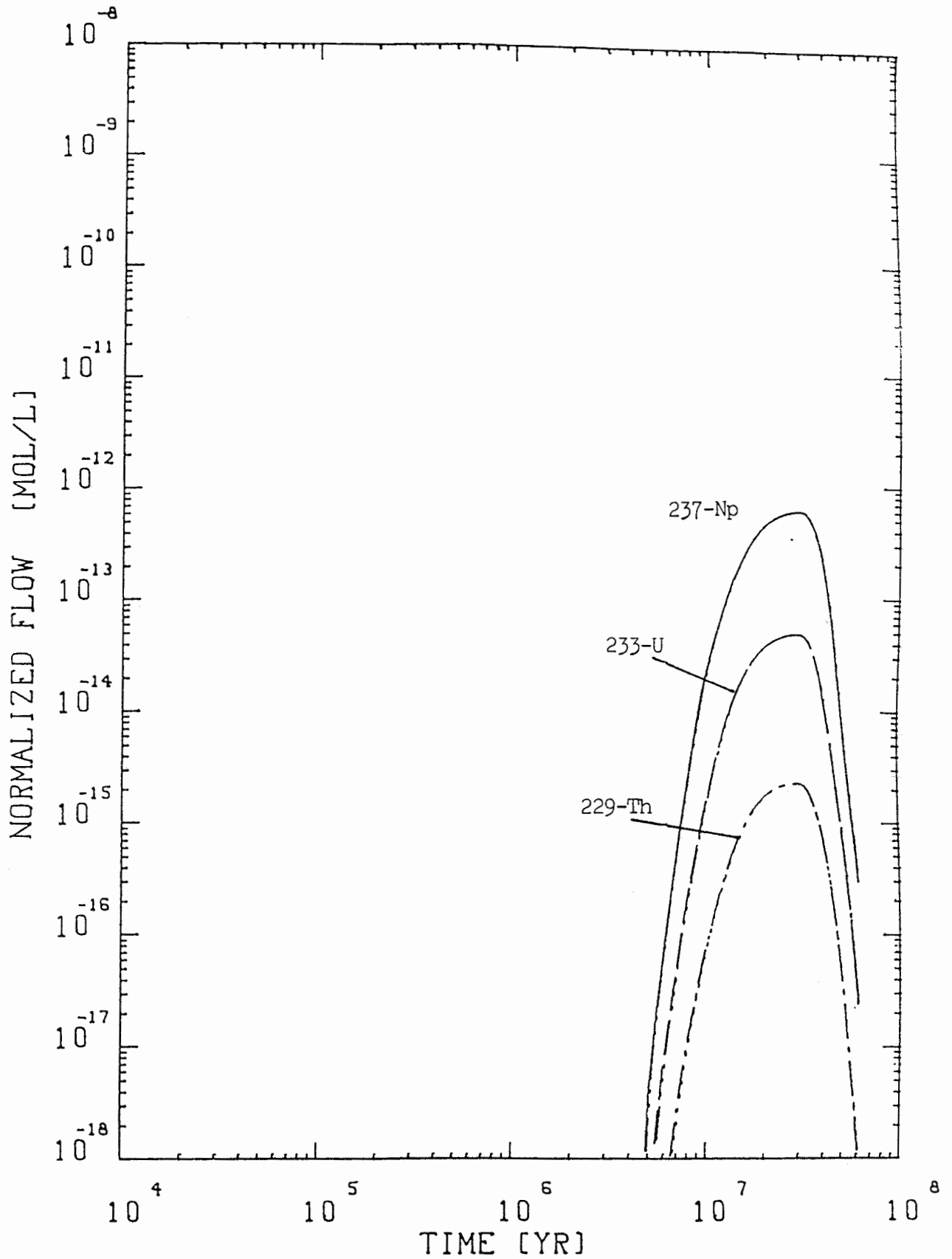case except for the fracture frequency (low value).

Figure 14   The same as figure 10. The parameters are the same as in the
base case except for the fracture frequency (low value),
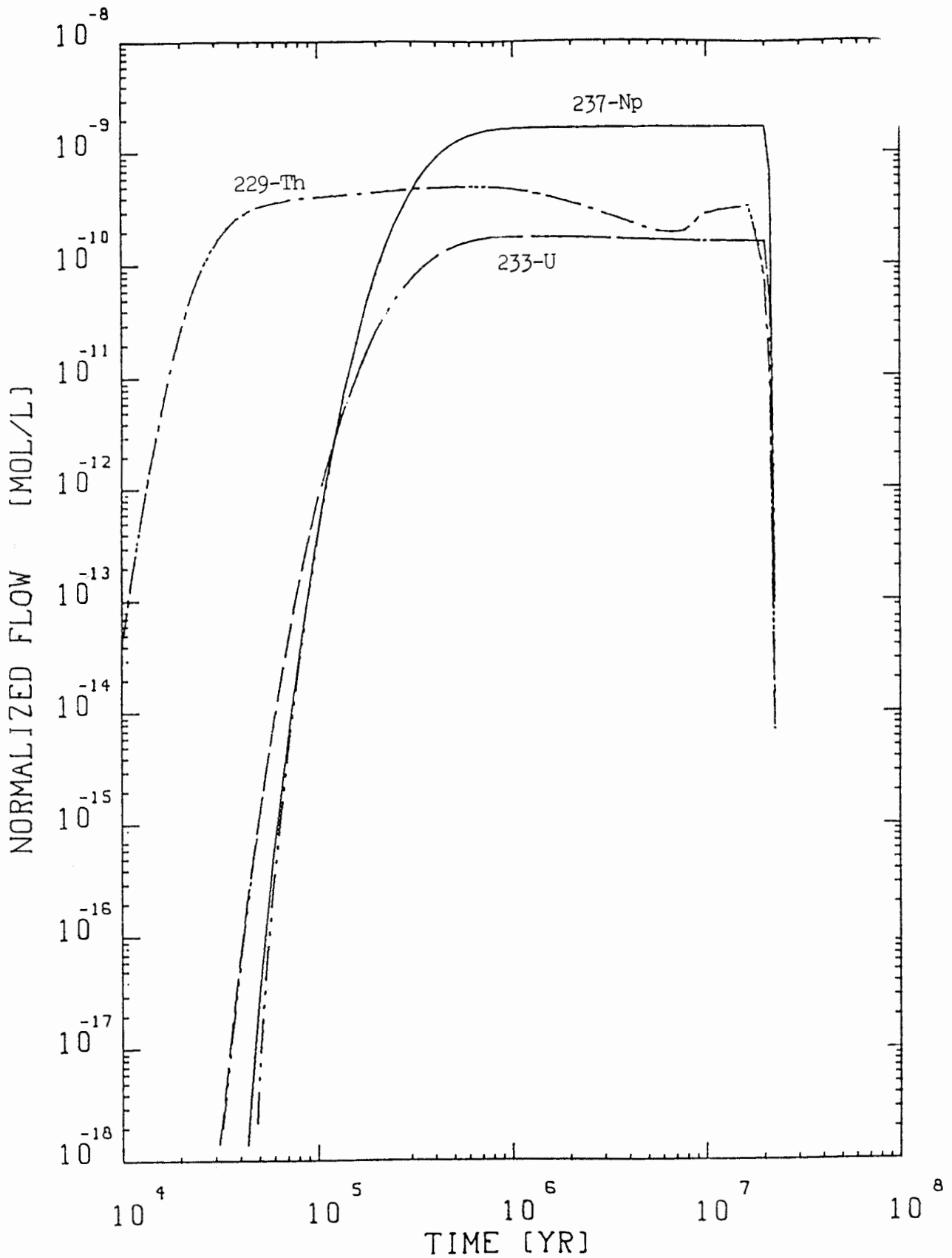diffusion constant (low value) and an increased width of
altered   zone (D = 0.01 m).

Figure 15 The same as figure 10. The parameters are those of the base case except for the fracture frequency (low value), diffusion constant (low value) and sorption constants (set of low values).
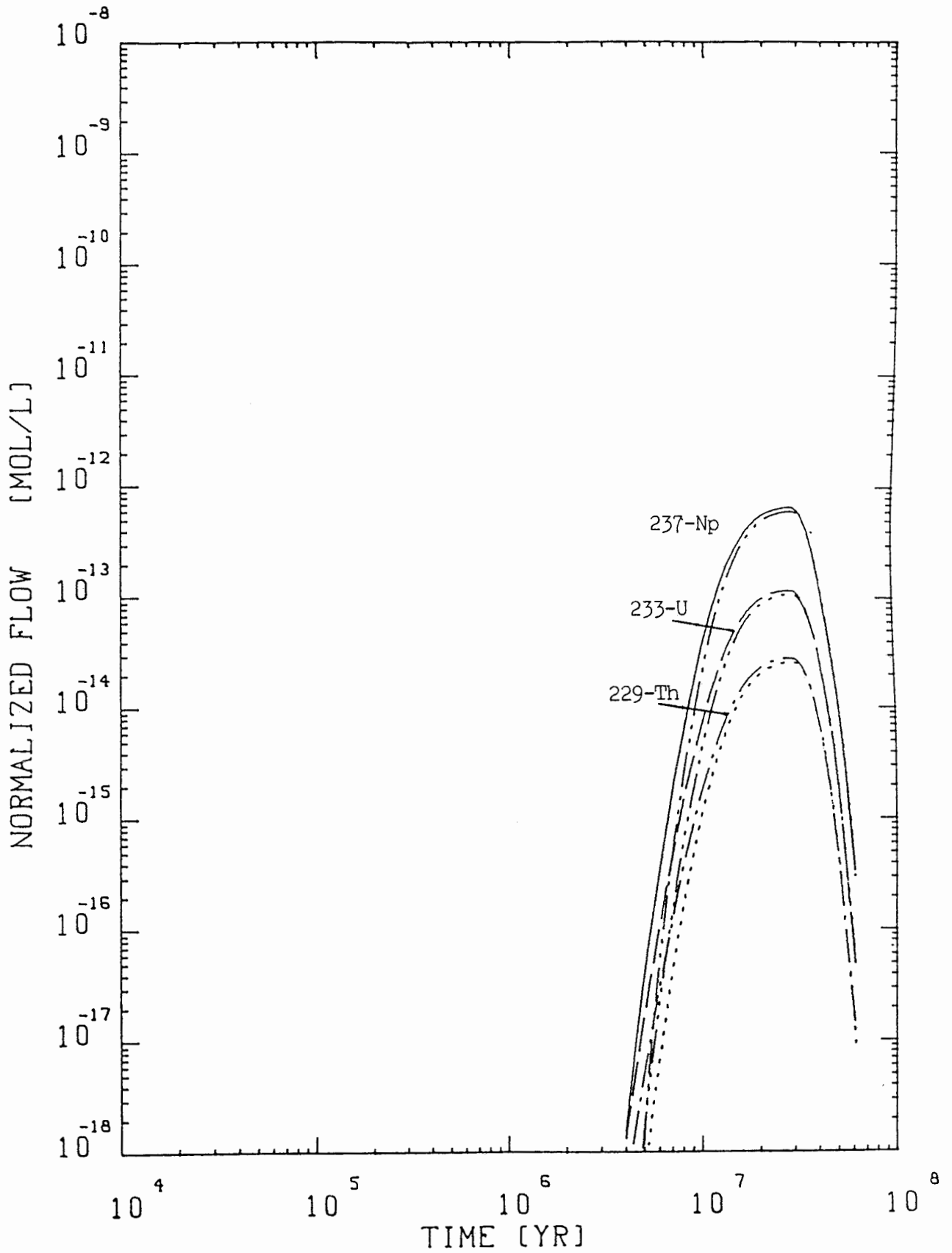
Figure 16   The same as figure 15 but with an increased width of the
             altered   zone (D = 0.1 m).